U.S.NRC
United States Nuclear Regulatory Commission
Protecting People and the Environment

RIL 2025-09

Technical Support for Analytical and Experimental Studies of Floating Seismic Isolation Systems

Date Published: September 2025

Prepared by:
M. Miah[1]
M. Tabbakhha[2]
D. McCallen[1]

[1]Lawrence Berkeley National Laboratory (LBNL)
[2]Currently at Thornton Tomasetti (formerly LBNL)

Jinsuo Nie, NRC Project Manager

Research Information Letter
Office of Nuclear Regulatory Research

Disclaimer

Legally binding regulatory requirements are stated only in laws, NRC regulations, licenses, including technical specifications, or orders; not in Research Information Letters (RILs). A RIL is not regulatory guidance, although NRC's regulatory offices may consider the information in a RIL to determine whether any regulatory actions are warranted.

FORWARD

Research Information Letter 2025-09, “Technical Support for Analytical and Experimental Studies of Floating Seismic Isolation Systems,” summarizes research conducted by Lawrence Berkeley National Laboratory (LBNL) under a contract with the Office of Nuclear Regulatory Research, Division of Engineering. This work was performed under the Memorandum of Cooperation (MOC) between the U.S. Nuclear Regulatory Commission (NRC) and the Japan Atomic Energy Agency (JAEA), signed in February 2023.

The study evaluates the feasibility of using LS-DYNA and OpenSeesPy to simulate the seismic performance of the Floating Seismic Isolation System (FSIS), a concept proposed by JAEA for small modular reactors. Through a series of benchmark analyses using simplified models and available test data, LBNL found that both simulation tools can effectively capture the fundamental mechanics and fluid-structure interaction (FSI) dynamics of FSIS. The study also highlights that OpenSeesPy would benefit from further development to support more advanced fluid and FSI modeling capabilities.

Importantly, the research confirms that the FSIS design features, including air cavities and orifices, are effective in reducing seismic demands in both horizontal and vertical directions. These findings are expected to inform future evaluations involving large-scale testing and FSIS design applications.

Technical Support for Analytical and Experimental Studies of Floating Seismic Isolation Systems

A Report to the Office of Nuclear Regulatory Research U.S. Nuclear Regulatory Commission

May 2025

BERKELEY LAB

Bringing Science Solutions to the World

Technical Support for Analytical and Experimental Studies of Floating Seismic Isolation Systems

Energy Geosciences Division
Lawrence Berkeley National Laboratory

Mamun Miah[1]
Maryam Tabbakhha[2]
David McCallen[1]

Sponsored by the Office of Nuclear Regulatory Research
U.S. Nuclear Regulatory Commission

May 2025

(Updated on September 17, 2025)

[1] Lawrence Berkeley National Laboratory
[2] Currently at Thornton Tomasetti (formerly LBNL)

1.0 EXECUTIVE SUMMARY

The ability to ensure robust resilience against earthquake motions is an essential requirement for all nuclear power plant systems (NPPs). There have been a number of innovative technologies that were proposed for seismic response modification for NPPs, including application of traditional seismic base isolation technologies to help ensure adequate earthquake performance. A new and unique response modification concept has recently been proposed to place a reactor system on a floating platform in a large water pool. The underlying principle includes exploitation of the fact that shear waves cannot propagate through water, and floating the reactor building on a reservoir of water can potentially isolate the reactor building from incoming earthquake-induced waves. Because the water can transmit compressional waves, the proposed system would reduce the seismic response from vertical motions by utilizing air cavities and damping inducing orifices. To explore the seismic performance of such a system, it is essential to have computational simulation models that can adequately represent the dynamic response of such a complex fluid-structure system.

The objective of the work described here is to provide the U.S. Nuclear Regulatory Commission with technical knowledge required to appropriately evaluate the seismic performance of this innovative isolation system. In this project, performances of two existing and readily available finite element software programs, namely LS-DYNA and OpenSeesPy, are critically evaluated in terms of their ability to appropriately represent the associated fluid-structure interaction phenomena and to estimate the transient response of the floating systems during earthquake induced motions. A suite of numerical tests aimed at verifying the capabilities, including gravity initialization, sloshing, and system transient response due to earthquakes, are described. Additionally, the degree of difficulty in the appropriate application of the software capabilities is commented on to provide the NRC with insights into the ability to use the identified simulation capabilities in regulatory confirmatory analyses.

TABLE OF CONTENTS

2.0 LIST OF FIGURES

3.0 LIST OF ABBREVIATIONS

ALE – Arbitrary Lagrangian Eulerian

DRM – Domain Reduction Method

EOS – Equation of State

FASSI - Fluid-Air-Structure-Soil Interactions

FE – Finite Element

FSI – Fluid-Structure Interaction

FSIS – Floating Seismic Isolation System

GPU – Graphical Processing Unit

JAEA – Japan Atomic Energy Agency

LBNL – Lawrence Berkeley National Laboratory

LS-DYNA – Livermore Software Technology Corporation's DYNA3D

MPI – Message Passing Interface

MPP – Massively Parallel Processing

NPP – Nuclear Power Plant

NRC – Nuclear Regulatory Commission

OpenSeesPy – Open-Source Earthquake Engineering Software in Python

PFEM - Particle Finite Element Method

SMR – Small Modular Reactor

SSI – Soil-Structure Interaction

USGS – United States Geological Survey

4.0 INTRODUCTION

The U.S. Nuclear Regulatory Commission, Office of Nuclear Regulatory Research (NRC/RES) is performing technical work to understand the performance of floating seismic isolation systems (FSIS) that are being proposed for small modular reactors. The NRC effort is in cooperation with the Japan Atomic Energy Agency (JAEA) and is focused on the exploration and development of computer models that can represent the dynamic response of fluid-isolated small modular reactors during earthquake events. The identified computer modeling capabilities would ultimately provide the NRC with the technical means to evaluate the seismic performance and safety of fluid- isolated small modular reactors during regulatory reviews.

The first phase of this project included the development and utilization of simple numerical simulation models and existing test data from JAEA to establish an analytical capability for simulating fluid-air-structure-soil-interactions (FASSI) under seismic loads. The NRC can utilize this work to develop modeling approaches and gain independent insight into the seismic performance of FASSI systems.

The FSIS concept under consideration has been developed and proposed by Yamamoto et al. [1]. The system consists of a small modular reactor placed inside a floating vessel in a pool of water as illustrated in Figure 1. The surrounding water is intended to isolate the reactor system from incident seismic shear (S) waves, which cannot propagate through water. To help attenuate incident compressional (P) waves (as they can transmit through water), an essential feature in the concept is the provision of air cavities with orifices that can provide augmented damping under seismic shaking. As the reactor building and reactor translate and rock under seismically induced displacements, changing the volume of the air cavities, air would be driven in and out through the large orifices in the air cavities, which is intended to provide a mechanism for added system energy dissipation.

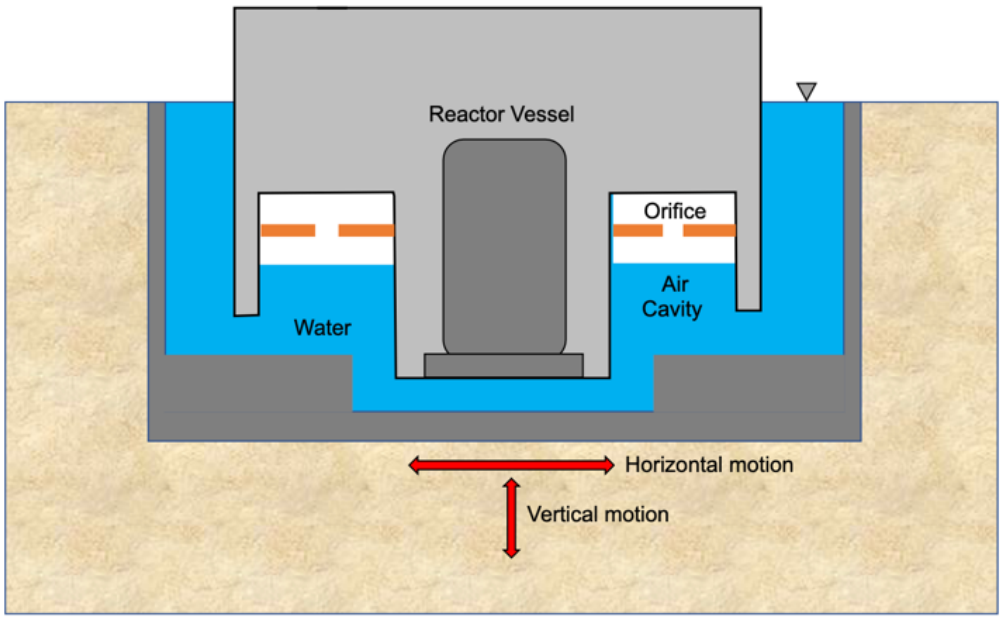

Figure 1. Small modular reactor floating seismic isolation system (FSIS) concept [1].

To fully characterize this system in a numerical model, it will be necessary to account for the interactions between the reactor building, the water, the air cavities and orifices, the pool and the surrounding soil which supports the entire engineered system. This requirement results in a need to develop a numerical model that represents the entire assembly as a coupled FASSI system. Given the fact that the system response, including the damping performance of the air cavities and orifices, is dependent on the system displacements and rotations, it will be desirable to develop a finite-displacement, geometrically nonlinear time domain model that fully tracks the system displacements in time.

This project explored two different finite element codes, LS-DYNA and OpenSeesPy, to evaluate their earthquake simulation capabilities for assessing the seismic performance of FSISs. The LS-DYNA software capabilities will be discussed first and then the OpenSeesPy capabilities will be discussed in the later part of the report.

5.0 SUMMARY OF SELECTED SOFTWARE CAPABILITIES (TASK 1)

The NRC Office of Nuclear Regulatory Research expressed interest in assessing the capabilities of two existing finite element programs relevant to the modeling and simulation of FASSI phenomena. Both finite element codes that were evaluated are well known and broadly utilized in both industrial and research applications.

The commercially available LS-DYNA [2] is an explicit time integration finite element program with advanced capabilities for modeling finite-deformation, geometric nonlinearity and material nonlinearity. Implicit time integration capabilities have also been implemented in the current version of LS-DYNA which can be more relevant to long-duration earthquake excitations. The analyses conducted in this report utilized the explicit method. LS-DYNA has a large suite of material constitutive models, advanced contact/impact capabilities, a mature library of nonlinear finite element technologies, and an Arbitrary Lagrangian Eulerian (ALE) technology for modeling fluid-structure interaction (FSI) problems. A literature review indicates that LS-DYNA has been validated and used successfully in numerous applications related to nuclear facilities, including earthquake simulations as well as FSI problems with some representative examples including:

- The evaluation of aircraft impact on nuclear power plant buildings [3]
- The seismic response of soil-structure-interaction (SSI) systems [4]
- FSI analysis for liquid-filled advanced reactors [5]
- Application to fluid sloshing in tanks [6-9]
- Application of floating boat and wave interaction which illustrate capabilities particularly relevant to the FASSI reactor system problem of interest [10]

The literature review of recent LS-DYNA applications in FSI indicated that the basic capabilities required to model floating reactor systems appear to be in place through an ALE/Lagrange coupling framework, as described in [11].

The work described herein was confirmatory in terms of investigating the ability to model FSIS specific phenomenon. LS-DYNA is a mature validated commercial software system and has the

benefit of an extensive user base, software question and answer support and software quality assurance which can be important in a regulatory application environment.

The second software package considered at the request of the NRC was the Python version of the well-known OpenSees program [12].

OpenSees [13] is an open-access program originally developed as a robust research code at the University of California, Berkeley, with the original focus on earthquake engineering applications. OpenSees is an implicit time integration code and has extensive structural elements, e.g., shell, plate, beam and column elements, as well as various solid elements formulations with particularly strong capabilities for practical structural engineering representation of the nonlinear response of reinforced concrete and steel structures. More recent developments include the implementation of nonlinear soil models and the implementation of the Domain Reduction Method (DRM) and Perfectly Matched Layers (PML) for time domain SSI analyses. In addition, for FSI problems a Particle Finite Element Method (PFEM) has been implemented in a Lagrangian framework. A literature review identified the descriptions of the PFEM development and representative example applications:

- Modeling fluid-structure interaction by the PFEM in OpenSees [14]
- Fluid-Structure Interaction and python-scripting capabilities in OpenSees [15]
- Application of OpenSees for tsunami loading on bridge superstructures [16]
- Wind-induced response of buildings incorporating nonlinear FSI effects [17]

Similar to LS-DYNA, the work described herein was confirmatory in terms of investigating the ability to model FSIS specific phenomenon with OpenSeesPy. OpenSeesPy is a mature validated open-source software system and has the benefit of an extensive user community that openly shares experiences and best practices. There is also the potential to work with the OpenSeesPy developers at the Oregon State University [18] to agilely and economically implement any special code features that might be needed in NRC confirmatory analyses.

6.0 LS-DYNA FEASIBILITY ANALYSIS (TASK 2)

6.1 MODELING APPROACHES IN LS-DYNA

LS-DYNA is a nonlinear, time-domain finite element software program successfully employed in earthquake simulations, including SSI [4] and FSI [5]. This software is one of the most widely used and reliable platforms to model fluid structure interaction in structural response related to civil engineering applications. The software's ability to simulate fluid dynamic phenomena, such as sloshing, has been verified by various authors [6-9]. Ensuring adequate and reliable results requires a thorough understanding of the underlying physics and skillful knowledge in appropriately representing the phenomena. Therefore, a comprehensive literature review is essential to ascertain the past applications of LS-DYNA in solving analogous problems.

6.2 FINITE ELEMENT MODEL DESCRIPTION

An Arbitrary Lagrangian Eulerian (ALE) formulation is used in this work to model FSI. This method combines elements of both Lagrangian and Eulerian formulations to address the challenges related to large displacements and deformations and FSI. This method allows tracking of material

interfaces over time which is crucial for fluid dynamics simulations. In this method, both air and water are modeled separately, and the interface between these fluids and the solid structure are defined independently. In all test models in this study, water and air were modeled using the Mat-Null constitutive material law, which is commonly employed for materials exhibiting fluid-like deformation characteristics like water and air. When used alone, it provides viscous stress in the material. When employed in conjunction with an Equation of State (EOS), this produces the deviatoric stress component, while the EOS contributes to the pressure component.

Table 1 presents the values utilized for describing the Mat-Null constitutive material law for water and air. The first-degree polynomial or the linear-polynomial equation of state is employed to model the pressure response of water, and air. For all cases the tank is assumed to be rigid. The interactions between the fluid and structures are modeled with a penalty type contact.

Table 1. The material properties of the fluids.

Material	Density (kg/m^3)	Dynamic Viscosity	Bulk Modulus (N/m^2)
Water	998	0.001	$2.2x10^9$
Air	1.18	0.00002	$1.01x10^5$

6.3 GRAVITY INITIALIZATION VALIDATION

When dealing with a substantial body of water, hydrostatic pressure becomes a crucial factor. Gravity is the primary force creating hydrostatic pressure in fluids and is applied by defining a body force. In this section, a numerical model is created to evaluate the software's accuracy in simulating gravity initialization and accurately calculating the hydrostatic pressure on the floating object. To assess this verification, the submerged height and buoyancy forces applied to the floating object are calculated and compared with hand calculations.

The numerical model consists of a rigid pool filled with water, featuring a floating object that undergoes gravity initialization. In this simulation, the body forces, representing the weight of the floating object, are applied incrementally over time to create a hydrostatic condition. In simulations involving water, the challenge arises from its highly incompressible nature, characterized by a high bulk modulus. Small changes in volume can lead to substantial pressure fluctuations, resulting in significant pressure oscillations. To address this issue, damping was assigned to the fluid via *DAMPING_PART_MASS to mitigate pressure oscillations. The damping was set to 30% and was determined by calculating the pressure oscillation period in the case where no damping was applied. The dimensions of the pool are 200 m in length, 100 m in width, and 150 m in depth. The water level within the pool is at a height of 100m. The block has a dimension of 24 m x 24 m x 16 m. Figure 2 presents a 3D view of the model.

A video was generated during the simulation, depicting the progressive stages of lowering the floating body into the water. The images at various time steps in Figure 3 depict the gravity initialization process, providing a comprehensive visual representation of the dynamic interaction between the floating body and water throughout the simulation. As depicted in these figures, the block is initially submerged in the water, and buoyancy forces subsequently bring it back to the surface, establishing an appropriate static equilibrium between the weight of the body and the

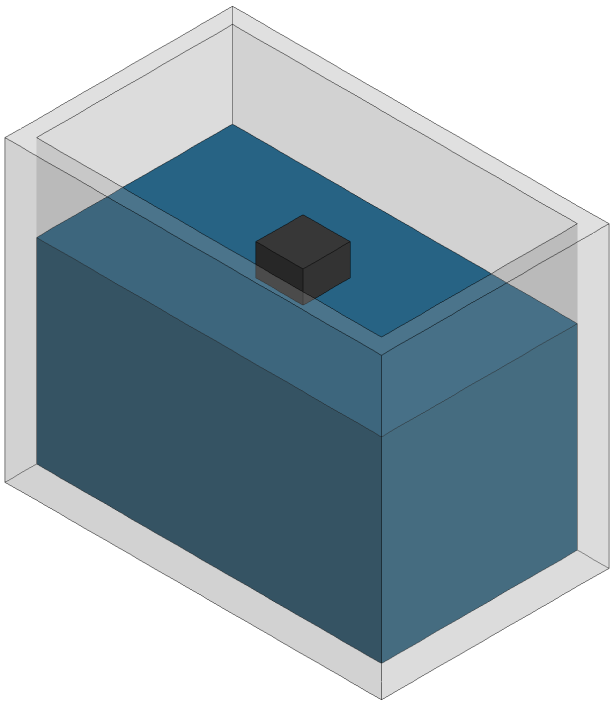

Figure 2. 3D numerical model test case for gravity initialization validation.

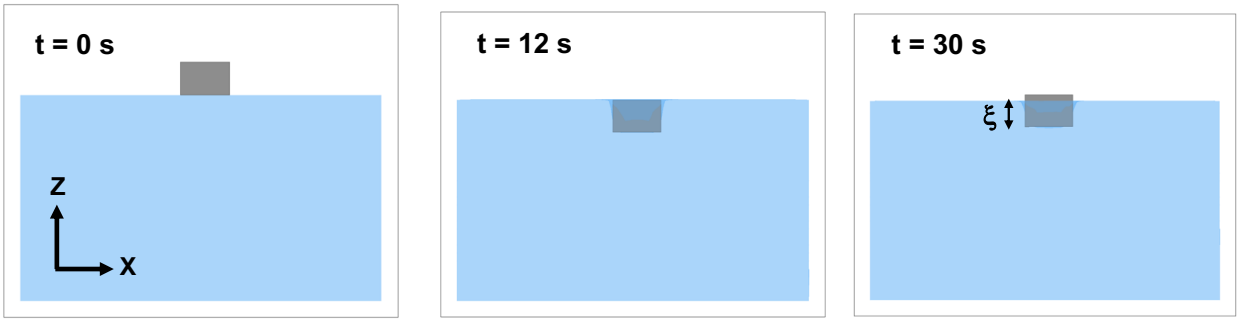

Figure 3. Sequential stages of gravity initialization process.

buoyancy force. Figure 4 displays ξ, the submerged height, as shown in Figure 3, over time. The final stabilized value on the curve is subsequently compared with the hand calculation for validation. The comparison reveals nearly identical results, indicating a high level of agreement between the two. Equation (1) presents the equilibrium equation for the floating box, where W represents the weight of the block, and F_b denotes the buoyancy forces acting on the block.

$$W = F_b \qquad (1)$$

Using Equation (1), the submerged height is calculated as 12.82 m, which is identical to the stabilized value obtained from the LS-DYNA numerical simulation, as depicted in Figure 4.

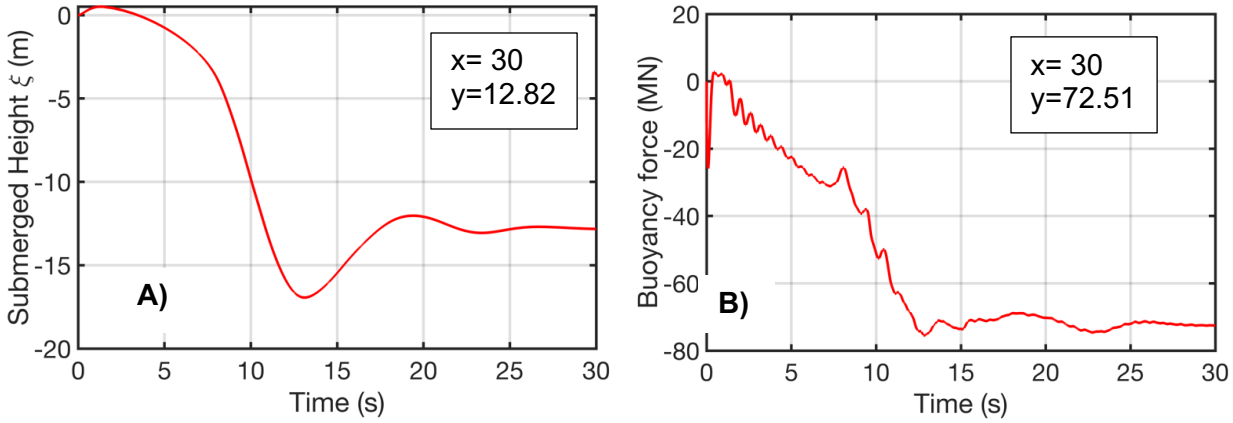

Figure 4. Submerged height and (B) buoyancy force variation over time.

Another verification was conducted to assess the accuracy of the buoyancy force acting in the Z-direction. Figure 4 illustrates the force along the Z-direction over time. The calculated buoyancy force was 72.32 MN (from Equation 1), while the simulation yields 72.51 MN. The close agreement between the hand-calculated and the simulated values demonstrates the reliable adequacy of the simulation in representing the gravity initialization process.

6.4 SLOSHING VERIFICATION OF THE FLUID MODEL IN LS-DYNA

In this section, the ability of the LS-DYNA software to simulate sloshing phenomena is evaluated. A 2D finite element model as detailed in the paper by Shao et al. [9], with dimensions of 1.73 m in length and 1.33 m in height, with a water height set at 0.5 m, is illustrated in Figure 5a. The fluid system, consisting of both air and water, is enclosed by a rigid tank. The element size is 1 cm throughout the entire model, resulting in 23,009 elements. The rigid tank movement is constrained in all dimensions except the x-direction. A horizontal velocity is applied to induce sloshing behavior as detailed in the paper by Shao et al. [9], where an experimental 10 second time history of wave height is provided. The tank's horizontal velocity (m/s) is expressed as:

$$V_t = 0.032 \cos(\frac{2\pi t}{T}) \qquad (2)$$

In Equation (2), T represents the period of motion, corresponding to 95% of the sloshing period of the fluid of 1.74 seconds, calculated based on Housner's formulation for rectangular systems [19]. Snapshots of the fluid movement, illustrating the sloshing behavior induced by the applied velocity at various time intervals, have been captured and illustrated in Figure 5. These serve as a visual depiction of the fluid's dynamic evolution, effectively presenting the captured sloshing behavior within the simulation.

Figure 6b illustrates the vertical displacement for point A, as presented in Figure 6a. The period of motion is identical to the calculated sloshing period which is 1.74 seconds. The analysis presented in this study including the fluid motion and the vertical displacement at point A, demonstrates the capabilities of LS-DYNA in simulating fluid sloshing behavior.

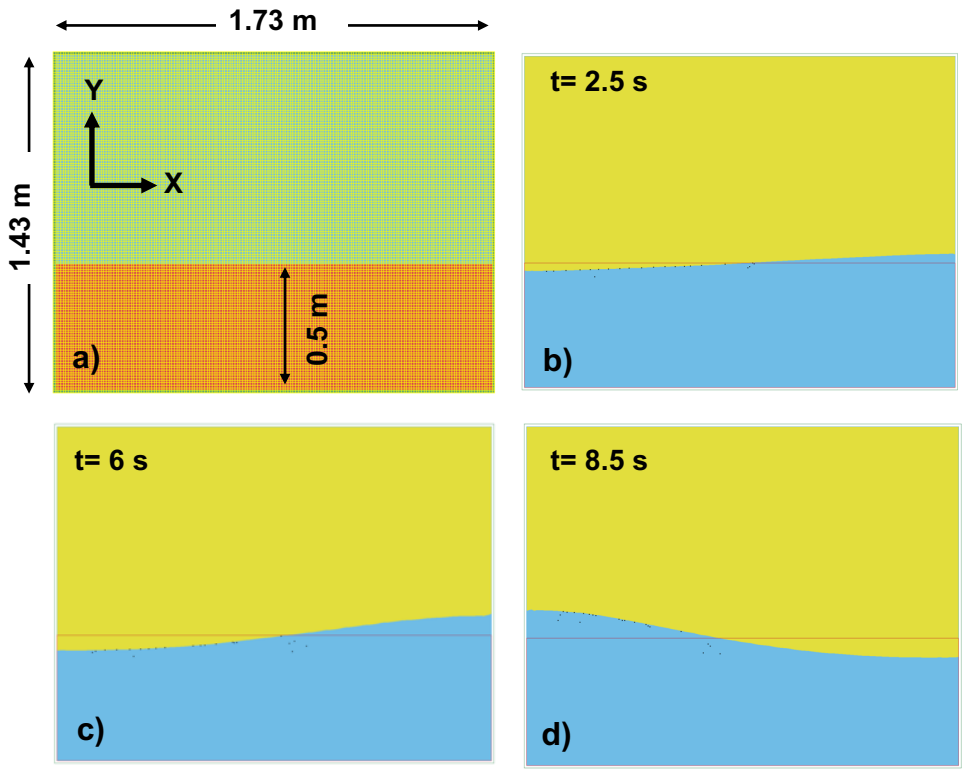

Figure 5. Dynamic evolution of fluid motion capturing sloshing phenomena.

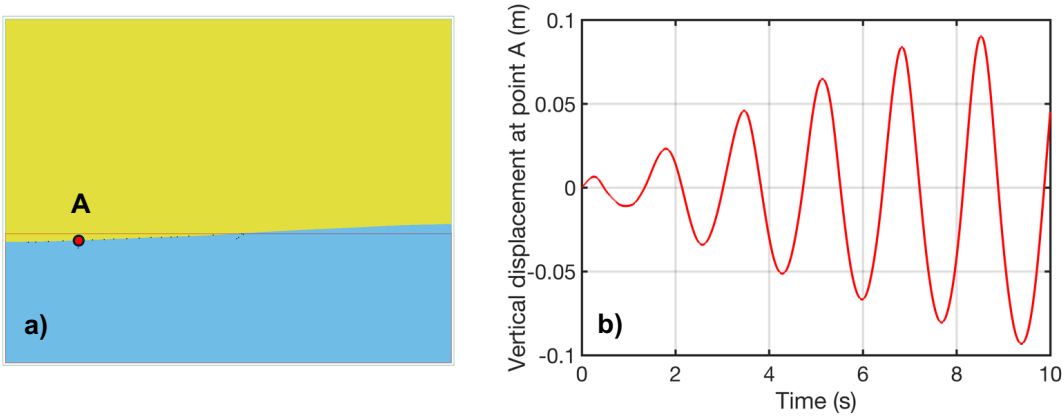

Figure 6. Vertical displacement of point A on the fluid surface.

6.5 INVESTIGATION OF WAVE REFLECTION

In this section, the investigation is focused on assessing the model's ability to adequately capture traveling and reflected waves. To achieve this, the model depicted in Figure 5a was utilized, and a horizontal pulse velocity function was applied at the tank base. This function began at zero velocity, steadily increased to a maximum of 1 m/s at 0.05 seconds, and then returned to zero velocity by 0.1 seconds as shown in the first figure. The corresponding variation of the water surface, depicted in Figure 7, spans from 0 to 1.3 seconds. Analysis of the water surface dynamics demonstrates the model's proficiency in adequately producing and reflecting surface waves.

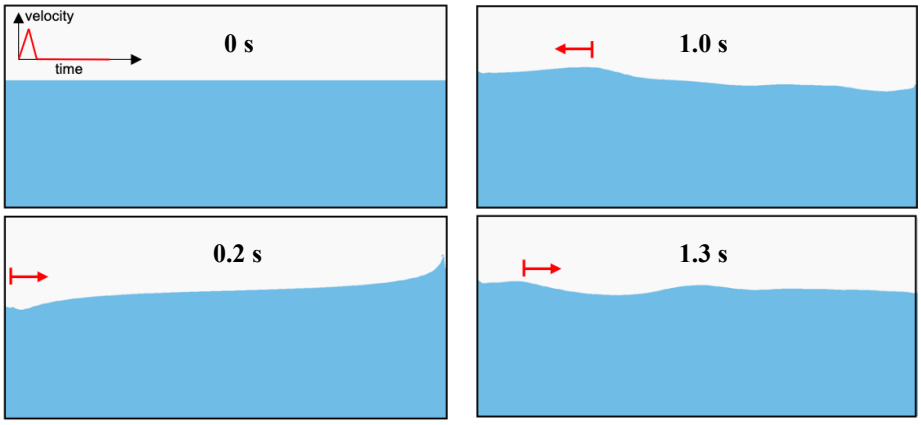

Figure 7. Demonstration of traveling and reflected waves in the water tank. (Note: it is the same model shown in Figure 5a. Aspect ratios look different due to not showing air and removing extra white space from top. It was confirmed by checking the aspect ratios of occupied water from two figures.)

6.6 EVALUATION OF SEISMIC RESPONSE OF THE FSI SYSTEM

In this section, the previously gravity-initialized system is subjected to a seismic excitation. Figure 8 displays the acceleration response spectra for a horizontal earthquake input excitation and the resulting response of the block. This earthquake motion was generated at Lawrence Berkeley National Laboratory (LBNL) using a high-performance geophysics model simulation [20,21]. A substantial reduction in the block's response in the corresponding direction is observed.

The provided snapshots in Figure 9 offer a detailed portrayal of the block's dynamic movement in response to earthquake excitation at various time steps, visually capturing the sequential and evolving behavior of the block, providing comprehensive insight into its response under seismic forces.

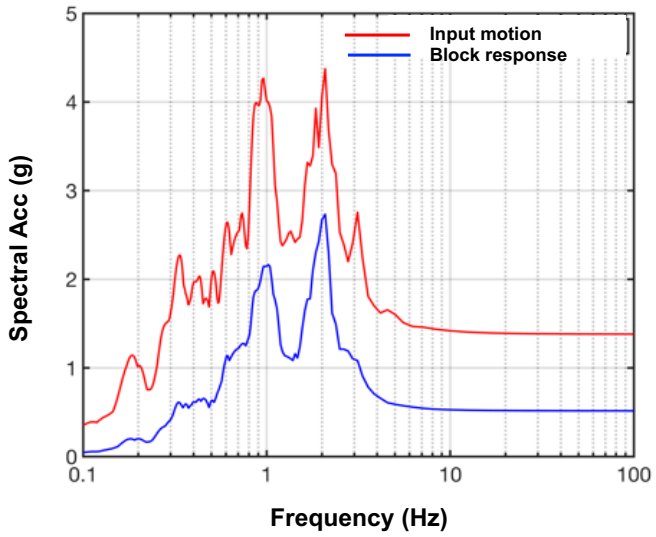

Figure 8. LS-DYNA demonstrates seismic response attenuation of the block under horizontal earthquake excitations.

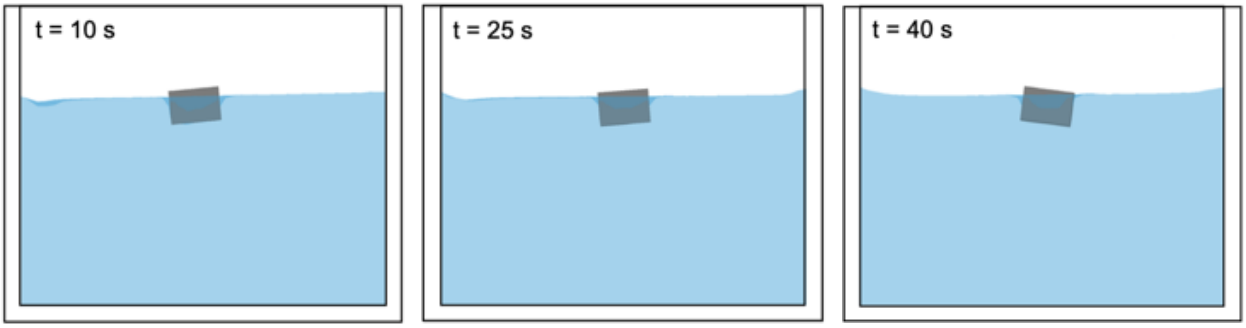

Figure 9. Sequential block movement during earthquake excitation at different time steps.

6.7 LS-DYNA SIMULATIONS OF THE JAEA SMALL SCALE EXPERIMENT

This section provides a short description of the JAEA small scale experimental tests described in the paper by Mori et al. [22]. The cited paper focuses on the FSIS technology for application to SMRs. The JAEA small scale experimental FSIS system consists of a pool of water with a small apparatus (i.e., representing a full scale NPP on 1/200 scale) floating in the pool. Both the apparatus and the container tank consist of aluminum (A5052), and weigh approximately 7.1 kg and 23 kg, respectively. In the tests, the water is adjusted so that the depth in the pool is 100 mm while the specimen is placed in the pool. Random wave excitation tests and seismic response tests are conducted to determine vibration and response characteristics of the specimen, respectively. Four types of tests are conducted – Type A (no air), Type B (air cavity), Type C (air cavity with 20 mm orifice), and Type D (air cavity with 10 mm orifice). Additional details of the tests, input earthquake excitations, and seismic response for four types of test conditions are described in the paper.

The specimen-pool-water system is subjected to earthquake excitations by placing it on an electromagnetic shaker table. The horizontal component of the earthquake excitation is mitigated by filtering through water, as water cannot transmit shear waves. To demonstrate vertical motion isolation the specimen has eight additional bottom air cavities that include orifices as a damping mechanism. The underlying physical mechanism provides a cushioning effect to the specimen by changing the trapped air volume (i.e., bulk modulus modification) during rocking from vertical earthquake excitations. The cushioning effect additionally induces a period elongation of the specimen response. Further, the presence of the orifices and their sizes are intended to provide increased damping ratios for response attenuation by letting air in and out through them during rocking of the system. However, the JAEA tests did not demonstrate much discernible difference in vertical motion isolation from orifice effects and LS-DYNA simulations are not performed for Type C and Type D tests.

In this section the seismic response for the JAEA small scale experimental specimen subject to vertical motions is evaluated using LS-DYNA (see Appendix A for details). The simulation results are compared with the experimental results published in the paper by Mori et al. [22]. Figure 10 illustrates the LS-DYNA ALE model for the JAEA experimental apparatus. The model consists of water at the bottom with the test specimen floating in the water. The ambient air starts from above the water surface and surrounds the specimen filling the air cavities. For clarity, the air is not shown in the model view. Two simulations are conducted for Type A and Type B tests as described in the paper by Mori et al. [22]. The Type A test consists of the specimen with all its

eight cavities filled with water and no trapped air. The Type B test consists of the specimen having its cavities filled with air first and then placed in water. The two test setups thus represent the effect of trapped air on the vertical seismic response attenuation of the FSISs. To represent these two types of tests in LS-DYNA simulations, the models are initialized in different ways.

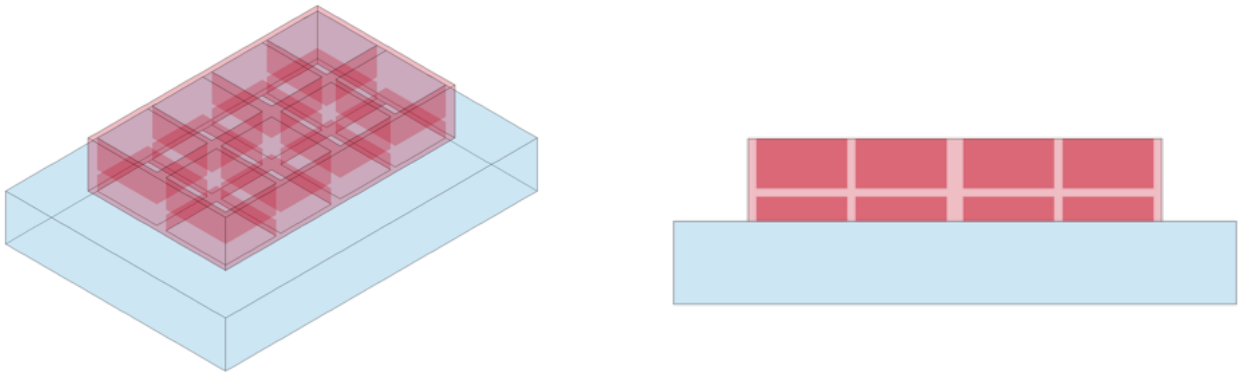

(a) Isometric view (b) Elevation view

Figure 10. LS-DYNA model for the JAEA small scale experiment – (a) isometric view and (b) elevation view.

Figure 11a demonstrates the Type A test where the specimen was initialized with its air cavities submerged in the water completely. Since the air in this model starts from above the water surface, this initialization ensures that there is no trapped air in the cavities. Figure 11b, on the other hand, demonstrates a model initialization where the specimen is placed right above water before the simulation starts, which ensures the cavities are filled with air before submerging into the water.

The input motion utilized for the vertical motion response simulation is shown in Figure 12. The LBNL team did not have access to the digital ground motion files used in the experiment, so the seismic input motion was collected from the National Research Institute for Earth Science and Disaster Resilience website [23] based on the referenced ground station. The motion was further processed and scaled according to the 1/200 scale similarity law utilized throughout the experiment. The total event simulation for both simulations is 2.5 seconds with a time step size 4.76e-6 seconds. The first 2.0 seconds are employed for gravity initialization of the FSI system after which an equilibrium state is achieved under gravity. Earthquake loading is applied thereafter for 0.5 seconds.

Figure 13 demonstrates results from the two simulations - for Type A in Figure 13a and Type B in Figure 13b. The response waveform frequencies for both types of tests demonstrate similarity with the input motion frequencies illustrated in Figure 12. Both simulation results indicate attenuation of the input motion. The Type A demonstrates a moderate amount of attenuation while the Type B indicates a significant amount of attenuation, indicating a notable cushioning effect that resulted from the compression of the entrained air volume during vertical movement of the

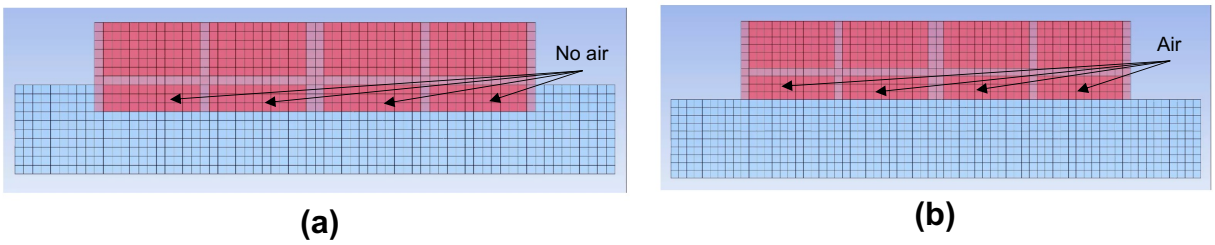

Figure 11. LS-DYNA model initializations for two types of tests conducted by JAEA – (a) Type A: air cavities completely filled with water and without trapped air and (b) Type B: cavities filled with trapped air.

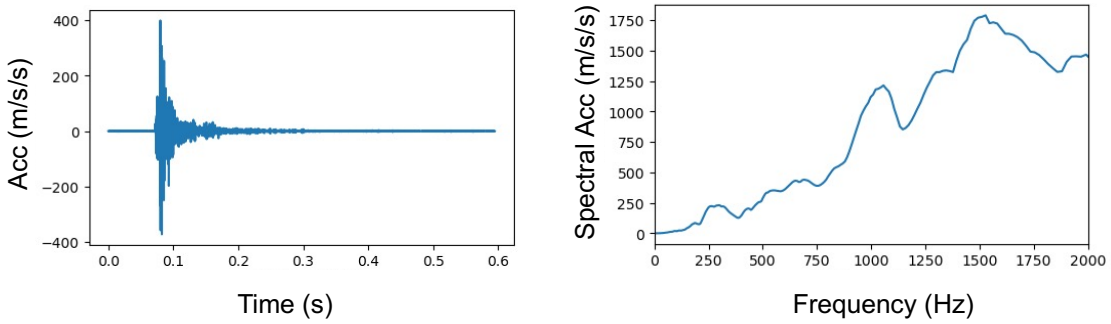

Figure 12. Earthquake input excitation utilized for vertical seismic isolation simulations in LS-DYNA – scaled according to 1/200 similarity law.

specimen. The simulation results are compared with the experimental results observed by the JAEA and illustrated in Figure 14. Red, blue, and gold curves indicate input motion, spectral response for Type A and spectral response for Type B tests, respectively. The paper also has Type C and Type D tests to consider orifices, for which the LS-DYNA simulations are not performed because we did not observe discernible difference in vertical motion isolation from orifice effects as reported in the paper. In general, the results indicate a very reasonable agreement for both Type A and Type B tests. However, for the Type A case, LS-DYNA simulation demonstrates a somewhat lower response above 1,500 Hz than the corresponding experimental results.

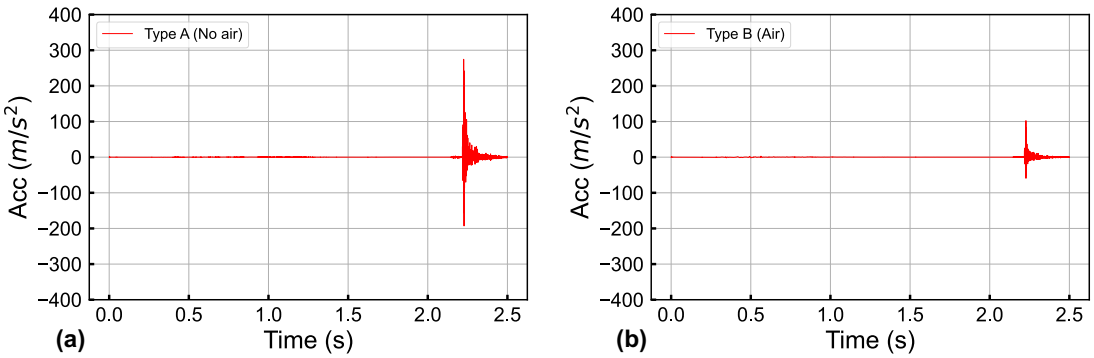

Figure 13. LS-DYNA simulation results for vertical seismic response of the JAEA small scale specimen for – (a) Type A and (b) Type B tests.

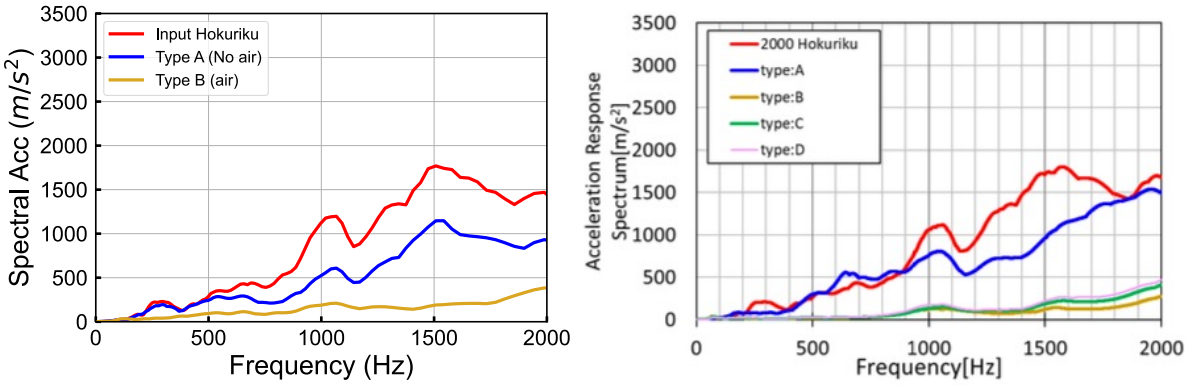

(a) Simulation results **(b) Experimental results**

Figure 14. Comparison of the vertical earthquake response results of the small-scale FSIS – (a) results from LS-DYNA simulations and (b) results from the JAEA experiment. The inclusion of the orifices (Type C and D) was not investigated in LS-DYNA.

7.0 OPENSEESPY FEASIBILITY ANALYSIS (TASK 2)

7.1 MODELING APPROACHES IN OPENSEESPY

OpenSeesPy is the Python version of the widely recognized OpenSees finite element software [15], a code extensively used in the open-source earthquake engineering research community. This code was extended [14] for simulating FSI behavior by implementing the PFEM approach. Due to its open-source nature and robust structural engineering modeling capabilities, an evaluation of the seismic performance of the proposed FSISs is conducted in this project. Similar to modeling approaches in LS-DYNA, first, a fluid sloshing demonstration is conducted in OpenSeesPy, followed by gravity initialization of the FSI system, and finally, concluded with the seismic response evaluation.

The PFEM has been shown to be an efficient approach to simulating FSI [24, 25]. The efficiency of the PFEM arises from its tracking of the fluid surface in Lagrangian form using a computational procedure analogous to that of traditional solid finite element formulations. OpenSeesPy employs a Lagrangian formulation for solving both structural and fluid simulations. For FSI simulations a Lagrangian formulation, as opposed to Eulerian formulation, can be advantageous as it can track the fluid free surface, and the approach is free of numerically difficult convective terms. Furthermore, under this FSI modeling approach, fluid formulation conforms to the Lagrangian formulations of structural mechanics.

7.2 FINITE ELEMENT MODEL DESCRIPTION

A 2D OpenSeesPy model of water within a tank is shown in Figure 15. The tank dimension is 0.5 m wide and 0.5 m in height. The water depth is 0.3 m. Figure 15 also illustrates the background particle meshing on the right. The fluid model consists of 'PFEMElementBubble' as element type in OpenSeesPy, with a density of 1,000 kg/m^3 and an element thickness of 0.012 m. The total

number of mesh particles is 54,000. This water-tank system is given a uniform base excitation to demonstrate the sloshing of water inside the tank.

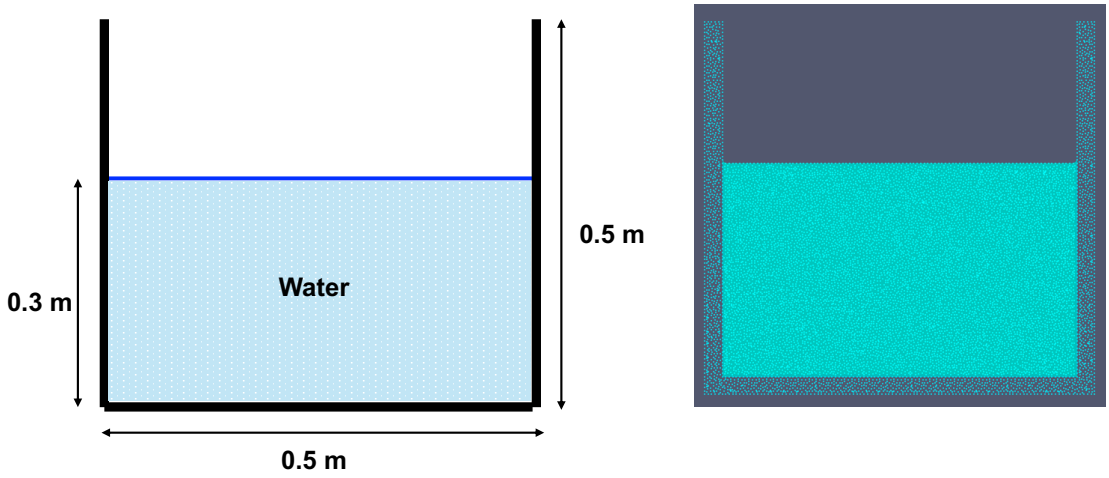

Figure 15. A 2D PFEM-based water-tank model in OpenSeesPy software framework.

7.3 SLOSHING VERIFICATION OF THE FLUID MODEL IN OPENSEESPY

Figure 16 exhibits three snapshots of water sloshing in the tank at three different times at 0 seconds, 2.6 seconds, and 3.1 seconds of the simulation. The plots clearly demonstrate water sloshing about its free surface with its fundamental mode. Figure 17 demonstrates a particle (marked with a red circle and labeled as A) at a distance of L/4 or 0.125 m from its boundary. The vertical motion of the particle A is tracked and plotted in Figure 17 on the right. The displacement time history plot of that particle demonstrates clear long-period oscillations about the free water surface marked at 0 m displacement. The plot also demonstrates a smooth and gradual decay of the particle displacement which resulted from the viscosity of the water, as there was no other damping mechanism applied to the system. The sloshing period is calculated as 0.8 seconds which matches closely with the analytical solution of 0.82 seconds [19].

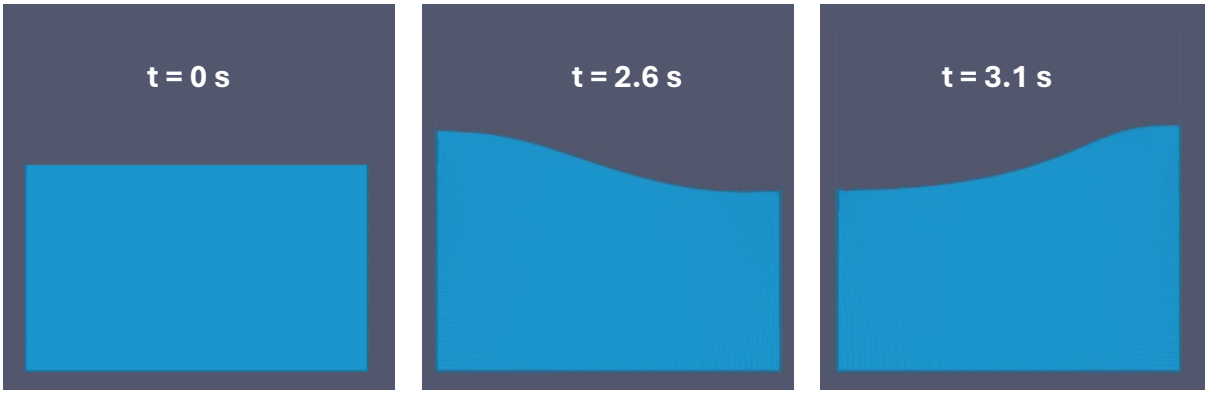

Figure 16. A successful demonstration of water sloshing in a water tank in OpenSeesPy.

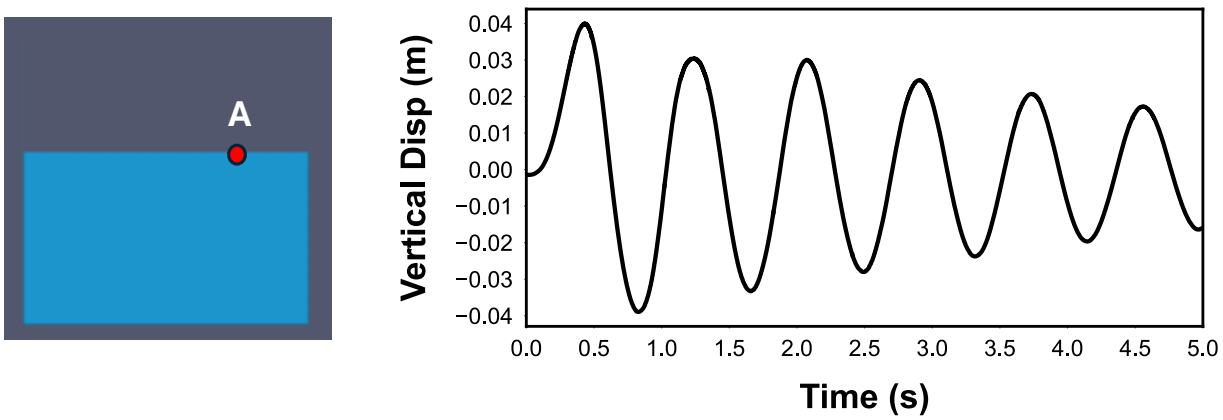

Figure 17. Displacement time history plot (right) for particle A (left) located on free water surface during sloshing.

7.4 GRAVITY INITIALIZATION OF AN FSI SYSTEM

Before running any dynamic analysis, it is essential to make sure that the FSI system under investigation is in equilibrium from preloaded gravity. A 200 m wide water tank with 150 m deep water is utilized and illustrated in Figure 18 (see Appendix B for implementation). A block with 24 m wide and 16 m height is placed on the free water surface. The FSI system is first initialized with gravity in an OpenSeesPy simulation before applying any earthquake excitations. The block response from the gravity initialization demonstrates sustained oscillations for an extended period without indicating substantial amount of response attenuation. There was no other damping applied to the system, this very low attenuation could be attributed to the low viscous fluid damping in OpenSeesPy or to some minor energy dissipation associated with the contact surface algorithms. To apply earthquake input motions, it is necessary to have the gravity response come to an equilibrium configuration. One option is to run the simulation for an extended period and then apply earthquake motions, which is computationally expensive. To avoid the long run time for the oscillatory behavior in OpenSeesPy, the submerged depth of the block under gravity equilibrium is calculated from the block's weight and the buoyant force (see Equation 1). The body is then manually placed very close to the actual static equilibrium position which reduces the gravity initialization simulation time significantly, since the initial position of the block starts from its near-equilibrium position from within the water. Several simulations are conducted to investigate the time sensitivity on gravity response attenuation before the block comes to an equilibrium state. This process has provided with the approximate time duration needed to equilibrate the gravity response before applying earthquake load. It is noted that the prolonged oscillation phenomenon was not observed in case of the block FSI simulations under ALE framework in LS-DYNA, and therefore, there was no need for adjustment in positioning of the block.

7.5 SEISMIC RESPONSE EVALUATION OF THE FSI SYSTEM

After accommodating an appropriate gravity initialization time for the FSI system, a horizontal earthquake excitation is applied to the system (see Appendix B for details). Figure 19 demonstrates gravity initialization time, earthquake input motions in red, and response of the solid block in blue.

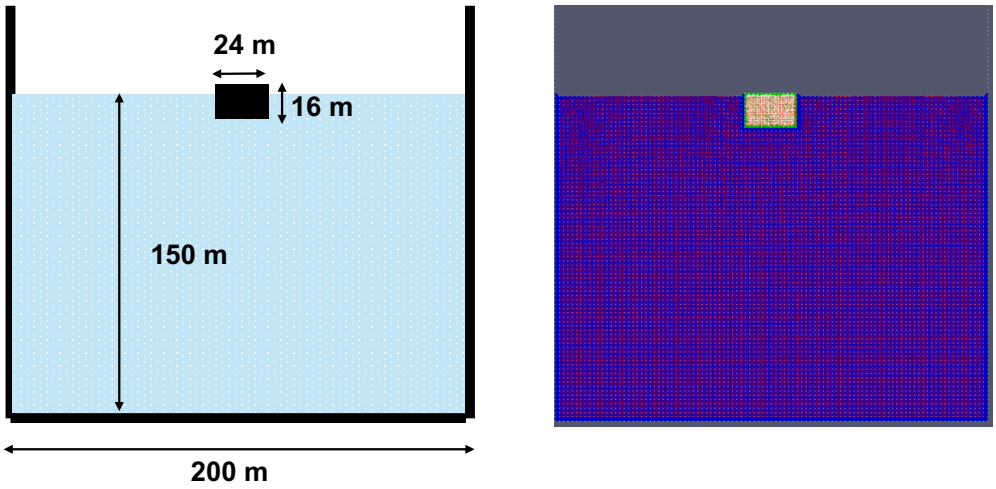

Figure 18. The dimensions of the FSI model and its simulation in OpenSeesPy.

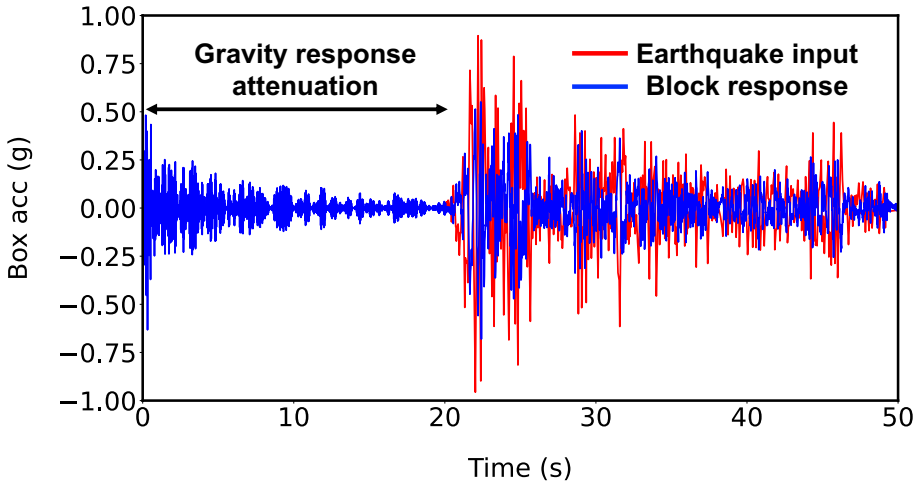

Figure 19. Demonstration of gravity initialization time for response equilibrium of the FSI system before applying earthquake excitations.

The response of the solid block indicates that nearly 20 seconds of gravity initialization time is required for the block to come to a near static equilibrium position. The block response during this period occurs predominantly in the vertical direction under the influence of gravity. However, some wobble-like oscillations are also noticed in the block, which most likely resulted from utilizing the PFEM method in OpenSeesPy. These wobbly block responses are reflected in Figure 19 between 0-20 s period. Earthquake excitations are applied at the end of the 20 seconds after this gravity response is diminished. The El Centro earthquake broadband motion is applied as horizontal excitation at the base of the water-tank system. One of the FSI simulations, where both gravity and earthquake excitations are applied simultaneously, demonstrates that gravity induces high-amplitude response to the FSI system in the higher frequency regime. The earthquake input motion and the block response from this simulation are plotted in Figure 20a, where high-amplitude responses are observed between 10-12 Hz. Figure 20b illustrates the FSI system response results from an alternative simulation, where gravity response has sufficiently subsided before responding to earthquake excitations. It is noted that the high-amplitude response of the block between 10-12 Hz has mostly been removed.

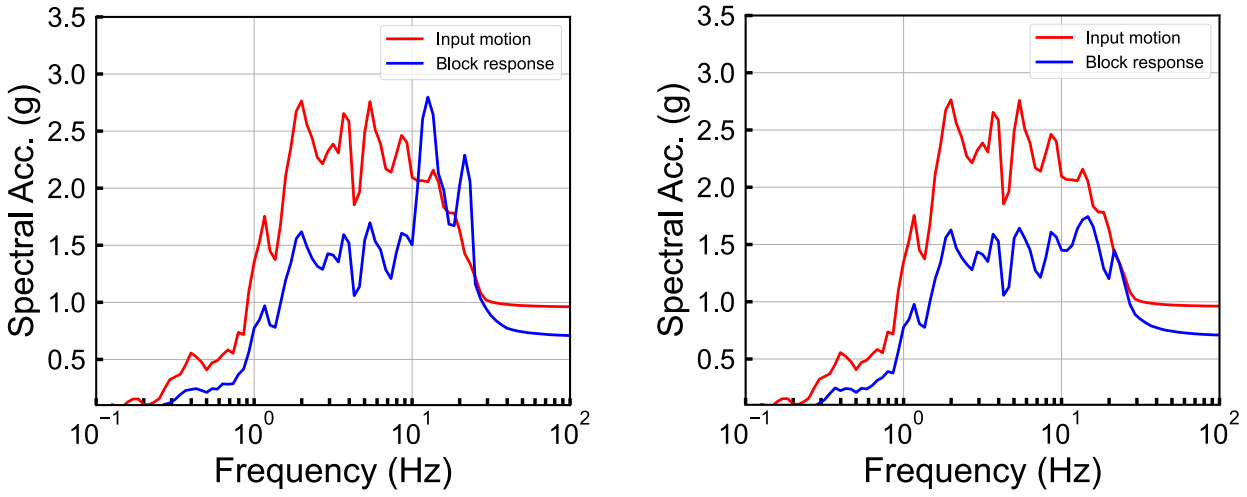

Figure 20. Demonstration of seismic attenuation of the block response from the El Centro horizontal earthquake input excitations – a) response without sufficient time duration for gravity initialization and b) response after gravity response has sufficiently subsided.

8.0 COMPARISON OF SEISMIC ATTENUATION

The seismic response results of the FSI system obtained from LS-DYNA and OpenSeesPy are compared and illustrated in Figure 21. The input motion for the LS-DYNA model was a synthetic ground motion (see Figure 21a) with 0-5 Hz frequency resolution whereas the input motion for the OpenSeesPy model was the El Centro earthquake broadband motion (see Figure 21b). Even though the input motions were different, the comparison demonstrates the horizontal seismic response attenuation achieved is on the same order for both models providing some confidence in the respective modeling approaches between the two different software platforms. FSI response from vertical input excitations were not conducted in OpenSeesPy due to time limitation and prioritization to conduct LS-DYNA simulations of the JAEA experimental tests.

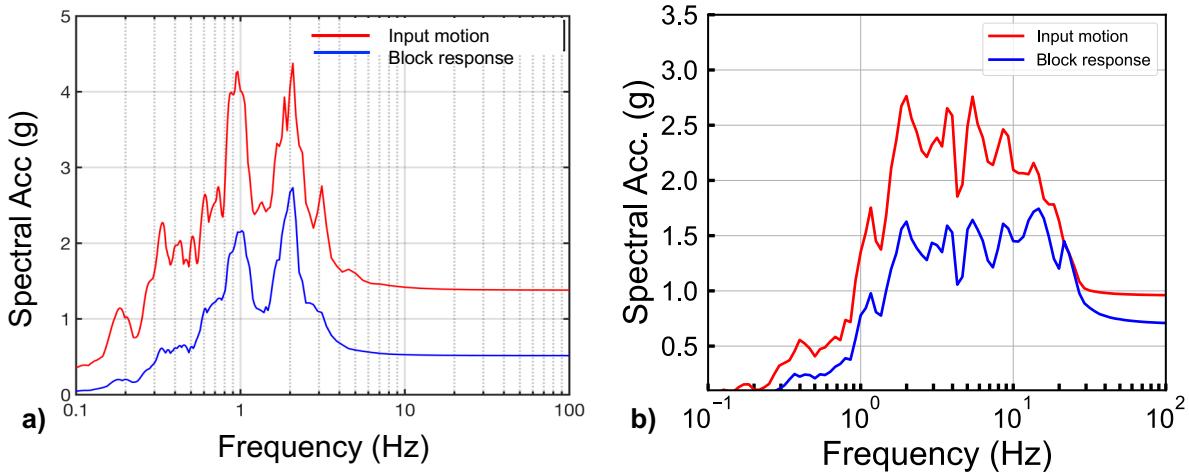

Figure 21. Comparison of horizontal seismic response attenuation of the FSI system between two software – a) LS-DYNA response with 0-5 Hz synthetic input motions and b) OpenSeesPy results with broadband El Centro input motions.

9.0 RECOMMENDATIONS FOR CONFIRMATORY ANALYSIS AND ADDITIONAL CONSIDERATIONS FOR SEISMIC RISK OF FLOATING MODULAR REACTORS

The ability of both LS-DYNA and OpenSeesPy to represent the fundamental mechanics associated with the concept of seismic isolation of an SMR immersed in a reservoir of water has been numerically demonstrated. In addition, LS-DYNA simulations for the JAEA small scale (1/200 of a full scale NPP) experimental tests [22] have been performed to demonstrate the isolation concept. It has been demonstrated that both codes can adequately capture fluid sloshing and FSI phenomena under seismic conditions. However, LS-DYNA has a more robust capability of defining coupling mechanisms between different types of materials (e.g., air, water, aluminum) as demonstrated in the JAEA small scale experiment simulations. LS-DYNA also benefits from many more user applications to FSI problems that have been tested and likely resulted in enhancements to the code. OpenSeesPy has some basic level coupling mechanisms between structural elements and water only. There are no other fluid materials developed in OpenSeesPy yet. Furthermore, to demonstrate sloshing in OpenSeesPy, several back-and-forth communications with the developers were made as fluid was observed leaking through the walls in sloshing simulation. The ALE methodology for fluid modeling is straightforward. Since OpenSeesPy is mainly a structural analysis code it requires additional developments to implement advanced fluid and FSI modeling features depending on the complexity of the FSI problems.

To ensure the U.S. NRC has a reliable and adequate tool for simulating reactor seismic performance for confirmatory analysis, it will be important to carefully validate numerical simulation results against experimental data from larger-scale experiments where the mechanics of the problem are closer to a full-scale FSIS reactor system. Comparisons of simulation predictions against experimental data will allow confirmation that selected model parameters, for example, penalty factors for the contact surfaces at material interfaces and the damping included in the numerical models, are representative of the actual physical systems.

It will be particularly important to calibrate the simulation model damping representation for these types of complex coupled systems which include orifices with fluid flow for enhancing damping levels. In addition, larger scale experiments should be used to carefully verify the ability of the designed orifices to enhance system damping. The most efficient damping that can be achieved by fluid being forced through an orifice tends to be relatively narrow band in terms of the frequency content of vibratory motion that realizes large amplitude reduction, and the practical damping realized can also depend on the amplitude of motion. In the system analysis of Yamamoto et al. [1] the frequency dependence of damping is illustrated. In the authors' experience in other applications, the realized damping can be less than the damping from an idealized model and thus damping needs careful experimental validation with appropriate attention to the frequency range in which damping reduces motions. It is noted that in the small-scale experiment that was performed, the damping realized from the addition of orifices for vertical excitation was insignificant [22].

Floating Reactor Tethering and Umbilical Components

In the available literature for this type of innovative floating reactor system, there is little detailed discussion or demonstration of how the floating reactor system will be tethered to prevent large reactor drift displacements and potential exceedance of available drift displacement limits.

Tensioning of any drift limiting tether system, with associated stiffening of restraints, or impact with the reservoir walls created by the large mass loading of sloshing fluid, could create a potential to induce significant loads to the floating system. In addition, drifts and motion of the reactor island must be addressed to appropriately design utility and umbilical connections to the island. This will require a careful analysis particularly when significant reservoir fluid sloshing can be induced by low frequency components of earthquake ground motions. These details will need to be defined and carefully represented in any future fully 3D reactor system model.

Long Period Motions

The focus of the engineering analyses found in the existing literature has been on the attenuation of high frequency components of earthquake ground motion, however careful analysis should be applied to the mechanism by which drift restraint is applied with full consideration of longer-period earthquake motions. Historical experience and recent regional simulations have indicated that long period motions (i.e., period > 1.0 s) generated by larger earthquakes can propagate to large distances and generate large vibratory motions in fluid systems. For example, large earthquakes in the western United States have illustrated the potential effects of low frequency ground motions at large distances from the epicentral region. Figure 22 illustrates two major earthquakes that occurred in Nevada and California respectively. The M 7.1 event in Nevada generated long-period motions in Sacramento, California approximately 322 km from the epicenter. These motions resulted in substantial damage to a large water storage facility with the destruction of facility concrete walls, beams and columns due to motions of the enclosed water [26]. Ground motion measurements in the vicinity indicated long duration sinusoidal type motions with period of vibration of approximately 6-7 seconds [26]. For the M 7.1 event in Northern California, the motions were generally not felt by people on the ground in Sacramento, but low

Figure 22. Two major western United States earthquakes that resulted in significant fluid sloshing and structural damage in Sacramento California at epicentral distances of 322 km and 350 km (map courtesy USGS).

frequency motions resulted in significant sloshing observed in swimming pools throughout the Sacramento region [27], providing additional evidence of the potential for significant fluid motions at very large distances from an earthquake epicenter. It is noted that sloshing effects can become quite extreme when the ground motion frequency matches that of a large pool of water as evidenced by pool sloshing in the Turkey earthquake of 2023 [28]. These western U.S. observations should be considered in the context of much higher seismic wave attenuation with distance in western U.S. geology. In the central and eastern U.S., the attenuation rates are much lower due to the competency of the geologic strata and ground motions can propagate to significantly larger distances as illustrated by the zones of felt motions for western, central and eastern U.S. earthquakes as show in Figure 23. This provides additional impetus for careful consideration of long period fluid sloshing effects for central and eastern U.S. sites, and the potential large drift motions for a floating reactor system.

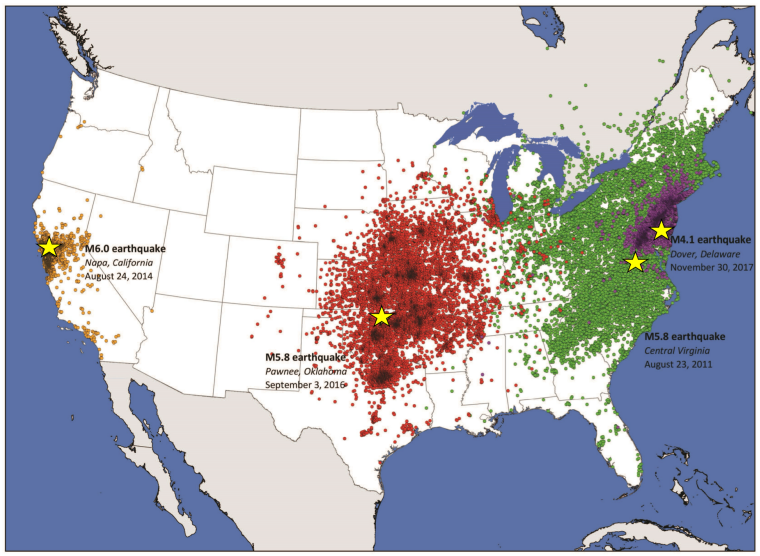

Figure 23. Zones of felt motions for M 6.0 western (brown dots), M 5.8 central (red dots), M 5.8 eastern (green dots) and M 4.1 eastern (purple dots) U.S. earthquakes (map courtesy USGS).

Further quantitative evidence of the long period motion effects has recently been obtained from new high-performance regional ground motion simulations as well as ground motion measurements at distance from major earthquakes. Figure 24 demonstrates ground motions in the Livermore Valley of California for a simulated M 7.5 earthquake on the San Andreas fault [29] along with measured ground motions in the Los Angeles basin due to the Landers California earthquake. Both the simulated and observed motions exhibit similar low frequency, large amplitude ground displacements at significant distance from the fault due to local basin response effects. These motions are shown in more detail in Appendix C.

Representation of Soil-Structure Interaction (SSI) in Full System Seismic Response

The combined mass of an SMR and water reservoir will be substantial, and the system will also likely have some degree of deep embedment into the surrounding supporting soil. SSI will ultimately need to be included for accurate representation of the seismic response of the full system.

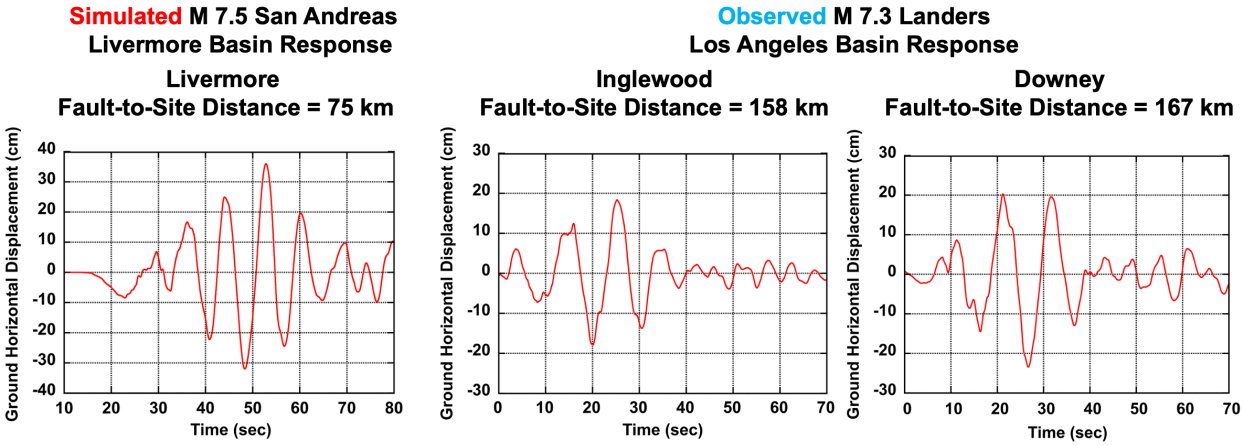

Figure 24. High amplitude, low frequency ground displacement time histories at large epicentral distances for major earthquakes.

It is noted that recent computational developments for the EQSIM fault-to-structure simulation framework allow appropriate coupling of regional geophysics wave propagation models with local soil-structure models through application of the Domain Reduction Method [30, 31]. This approach rigorously connects the larger geophysics domain with a local soil-structure system and fully represents complex incident seismic waves, including inclined body waves and surface waves, and soil-structure interaction. The DRM framework in EQSIM has already been linked to LS-DYNA and it would be straight forward to develop a full 3D model that includes the reactor system, water reservoir and surrounding soil.

Extending to Full 3D System Models on a Distributed Computing System

The computational technologies explored in the current study can readily be extended to a full 3D system model of a reactor system, but the computational demands will be substantial. It will be necessary to partition the full model domain for execution in parallel on a distributed computing system. LS-DYNA has rigorous capabilities for massively parallel computations, and it will just be necessary to execute such simulations on a sufficiently large, distributed computing platform.

10.0 SUMMARY AND CONCLUSIONS

The initial phase of this study involved a critical evaluation of existing finite element (FE) software programs, specifically assessing their capability to accurately estimate the transient response of floating isolation systems and simulate FASSI subjected to seismic loads. The preliminary results of the FSISs simulations were presented at an internationally recognized technical forum [32] and received significant attention among the experts and conference participants, indicating a great interest in FSISs simulations.

The scope of this report focused on the seismic simulation capabilities for SMR floating seismic isolation systems by utilizing two different carefully researched FE modeling approaches – the ALE modeling approach in LS-DYNA and Lagrangian modeling approach in OpenSeesPy. Both modeling approaches started by simulating fluid sloshing behavior and verifying the computed sloshing periods with analytical solutions, which was pivotal for investigating the seismic response of an FSI system. It was noted from the gravity initializations of the FSI systems

in both models that sufficient time needs to be allocated for the system responses to reach their equilibrium states before applying earthquake excitations.

The results from the earthquake excitations to the respective FSI systems indicated similar horizontal seismic response attenuation computed using two different numerical approaches in two codes. Furthermore, the strong agreement between the LS-DYNA simulation results and the experimental results for the JAEA small scale specimen provided confidence in subsequent modeling of large-scale FSIS problems, specifically for vertical earthquake excitations that involve FASSI-type coupling interactions.

The overall findings provided evidence that both LS-DYNA and OpenSeesPy software technologies can capture the fundamental mechanics and coupling dynamics of the FSI systems, laying a foundation for subsequent phases of the project and affirming the suitability of the codes for simulating intricate fluid-structure interactions in seismic environments. Additionally, OpenSeesPy would benefit from further developments to implement advanced fluid and FSI modeling features depending on the complexity of the FSI problems.

SOFTWARE VERSIONS

LS-DYNA MPP Double Precision R15.0.2-2 SSE2 Intel MPI 2018 is running on Rocky Linux 8 on LR7, and Centos7 on seismo3.

The Laboratory Research Computing program provides Lawrencium, a 942-node (23,424 computational cores) Linux cluster to its researchers needing access to computation to facilitate scientific discovery. The system, which consists of shared nodes and PI-contributed Condo nodes is equipped with an InfiniBand interconnect and has access to a 1.8 PB parallel filesystem storage system. Large memory, GPU, Intel and AMD nodes are also available.

ACKNOWLEDGMENTS

The HPC simulations conducted in this project utilized the Lawrencium Supercluster at LBNL. The essential system support from the Lawrencium Supercluster team is greatly acknowledged. Additionally, the technical advice on FSI coupling provided by an LS-DYNA expert, Ian Do, at Ansys, is greatly appreciated. The developers of the OpenSeesPy PFEM code, Minjie Zhu and Michael Scott, at Oregon State University, have been very helpful at various stages of the FSI simulations. On top of providing technical guidance, they frequently met with the LBNL team and navigated through the details of implementing the FSI simulations demonstrated in this report. Their contributions are greatly acknowledged.

REFERENCES

1. Yamamoto, T., Yan, X., Shimada, T., Motegi, H., Kai, S., Otani, A. (2022). Study on floating seismic isolation building for SMR. In *Proceedings of the 26th National Symposium on Power and Energy Systems*, Saga-ken, Japan, July 13-14, 2022.
2. Welcome to the LS-DYNA Product Space. https://lsdyna.ansys.com/

3. Li, Z. R., Li, Z. C., Dong, Z. F., Huang, T., Lu, Y. G., Rong, J. L., Wu, H. (2021). Damage and vibrations of nuclear power plant buildings subjected to aircraft crash part II: Numerical simulations. *Nuclear Engineering and Technology*, 53(9), 3085-3099.
4. Nguyen, K. T., Kusanovic, D. S., Asimaki, D. (2022). Three-dimensional nonlinear soil–structure interaction for Rayleigh wave incidence in layered soils. *Earthquake Engineering & Structural Dynamics*, 51(11), 2752-2770.
5. Yu, C. C., and Whittaker, A. S. (2021). Verification of numerical models for seismic fluid-structure interaction analysis of internal components in liquid-filled advanced reactors. *Earthquake Engineering & Structural Dynamics*, 50(6), 1692-1712.
6. Kozak, A. L., Tehrani, P. K., Abrahamson, T. E., Krimotat, A. V. (2016). Validation of the ale methodology by comparison with the experimental data obtained from a sloshing tank. In *14th International LS-DYNA Users Conference*.
7. Arafa, M. (2006). Finite element analysis of sloshing in liquid-filled containers. *Production Engineering and Design for Development (PEDD'07)*, 793-803.
8. Xu, J., Wang, J., Souli, M. (2015). SPH and ALE formulations for sloshing tank analysis. *The International Journal of Multiphysics*, 9(3), 209-224.
9. Shao, J. R., Li, H. Q., Liu, G. R., Liu, M. B. (2012). An improved SPH method for modeling liquid sloshing dynamics. *Computers & Structures*, 100, 18-26.
10. Wave modelling with LS-DYNA. https://www.youtube.com/watch?v=pObcA85SrmY
11. LS-DYNA ALE & Fluid-Structure Interaction Modeling. https://ftp.lstc.com/anonymous/outgoing/support/FAQ_docs/ale_overview_short2.pdf
12. OpenSeesPy. https://openseespydoc.readthedocs.io/en/latest/src/designsaferun.html
13. McKenna, F., Scott, M. H., Fenves, G. L. (2010). Nonlinear finite-element analysis software architecture using object composition. *Journal of Computing in Civil Engineering*, 24(1), 95-107.
14. Zhu, M., and Scott, M. H. (2014). Modeling fluid–structure interaction by the particle finite element method in OpenSees. *Computers & Structures*, 132, 12-21.
15. Zhu, M. and Scott, M. H. (2019). *Fluid-Structure Interaction and Python-Scripting Capabilities in OpenSees* (Report No. 2019/06). Pacific Earthquake Engineering Research Center (PEER). https://doi.org/10.55461/VDIX3057
16. Zhu, M., Elkhetali, I., Scott, M. H. (2018). Validation of OpenSees for tsunami loading on bridge superstructures. *Journal of Bridge Engineering*, 23(4), 04018015.
17. Ghaffary, A. and Moustafa, M. (2021). Wind-induced response of buildings incorporating nonlinear fluid-structure interaction effects. In *Proceedings of the 6th American Association for Wind Engineering Workshop*, pp. 238-244.
18. Michael H. Scott, PhD. https://web.engr.oregonstate.edu/~mhscott/
19. Housner, G.W. (1963). Dynamic analysis of fluids in containers subjected to acceleration. *Nuclear Reactors and Earthquakes, Report No. TID*, *7024*.

20. McCallen, D., Petersson, A., Rodgers, A., Pitarka, A., Miah, M., Petrone, F., Sjogreen, B., Abrahamson, N., Tang, H. (2021). EQSIM—A multidisciplinary framework for fault-to-structure earthquake simulations on exascale computers part I: Computational models and workflow. *Earthquake Spectra*, 37(2), 707-735.

21. McCallen, D., Petrone, F., Miah, M., Pitarka, A., Rodgers, A., Abrahamson, N. (2021). EQSIM—A multidisciplinary framework for fault-to-structure earthquake simulations on exascale computers, part II: Regional simulations of building response. *Earthquake Spectra*, 37(2), 736-761.

22. Mori, T., Shimada, T., Kai, S., Otani, A., Yamamoto, T., Yan, X.L. (2023). Experiment of floating seismic isolation system. In *Proceedings of the ASME 2023 Pressure Vessels & Piping Conference PVP2023-102224*. July 16-21, 2023, Atlanta, Georgia, USA.

23. NIED. (2019). NIED K-NET, KiK-net, National Research Institute for Earth Science and Disaster Resilience. https://doi.org/10.17598/nied.0004

24. Oñate, E., Idelsohn, S. R., Celigueta, M. A., Rossi, R., Marti, J., Carbonell, J. M., ... Suárez, B. (2011). Advances in the particle finite element method (PFEM) for solving coupled problems in engineering. *Particle-based methods: fundamentals and applications*, 1-49.

25. Idelsohn, S. R., Del Pin, F., Rossi, R., Oñate, E. (2009). Fluid–structure interaction problems with strong added-mass effect. *International Journal for Numerical Methods in Engineering*, 80(10), 1261-1294.

26. Steinbrugge, K. and Moran, D. (1957). Engineering aspects of the Dixie Valley-Fairview Peak earthquakes, Bulletin of the Seismological Society of America, 47(4), 335-348.

27. AP News. (2024, December 5). *Watch as water sloshes in swimming pools during California quake*. https://apnews.com/video/california-earthquakes-oregon-9b75cefcd73b47e4b36cefe4b04b6912

28. SahilOnline TV news. (2023, February 28). *CCTV footage showing swimming pool during recent Turkey earthquake* [Video]. YouTube. https://www.youtube.com/watch?v=r8p6QOE6uU0

29. McCallen, D., Pitarka, A., Tang, H., Pankajakshan, R., Petersson, N.A., Miah, M., Huang, J. (2024). Regional-scale fault-to-structure earthquake simulations with the EQSIM framework: Workflow maturation and computational performance on GPU-accelerated exascale platforms. *Earthquake Spectra*, 40(3), 1615-1652.

30. McCallen, D., Tang, H., Hu, S., Eckert, E., Huang, J., Petersson, N.A. (2022). Coupling of Regional Geophysics and Local Soil-Structure Models in the EQSIM Fault-to-Structure Earthquake Simulation Framework. The International Journal of High Performance Computing Applications, 36(1), 78-92. doi:10.1177/10943420211019118

31. McCallen, D., Pitarka, A., Tang, H., Pankajakshan, R., Petersson, N.A., Miah, M., Huang, J. (2024). Regional-scale fault-to-structure earthquake simulations with the EQSIM framework: Workflow maturation and computational performance on GPU-accelerated exascale platforms. Earthquake Spectra, 40(3), 1615-1652. doi:10.1177/87552930241246235

32. Tabbakhha, M., McCallen, D., Miah, M., Nie, J., Wang, W., Graizer, V., Pires, J., Bauer, L. (2024). Verification of earthquake simulation capabilities for small modular reactor (SMR)

floating seismic isolation systems. In *Pressure Vessels and Piping Conference* (Vol. 88513, p. V005T08A008). American Society of Mechanical Engineers.

Appendix A – Modeling Features Utilized in LS-DYNA

LS-DYNA MODELING FEATURES USED FOR THE JAEA FSIS EXPERIMENT SIMULATIONS

In the following section the LS-DYNA modeling features used for the JAEA small-scale experiment simulation are described. Figure A11 demonstrates the JAEA small-scale experimental model setup in LS-DYNA and the relevant keywords used for the simulations.

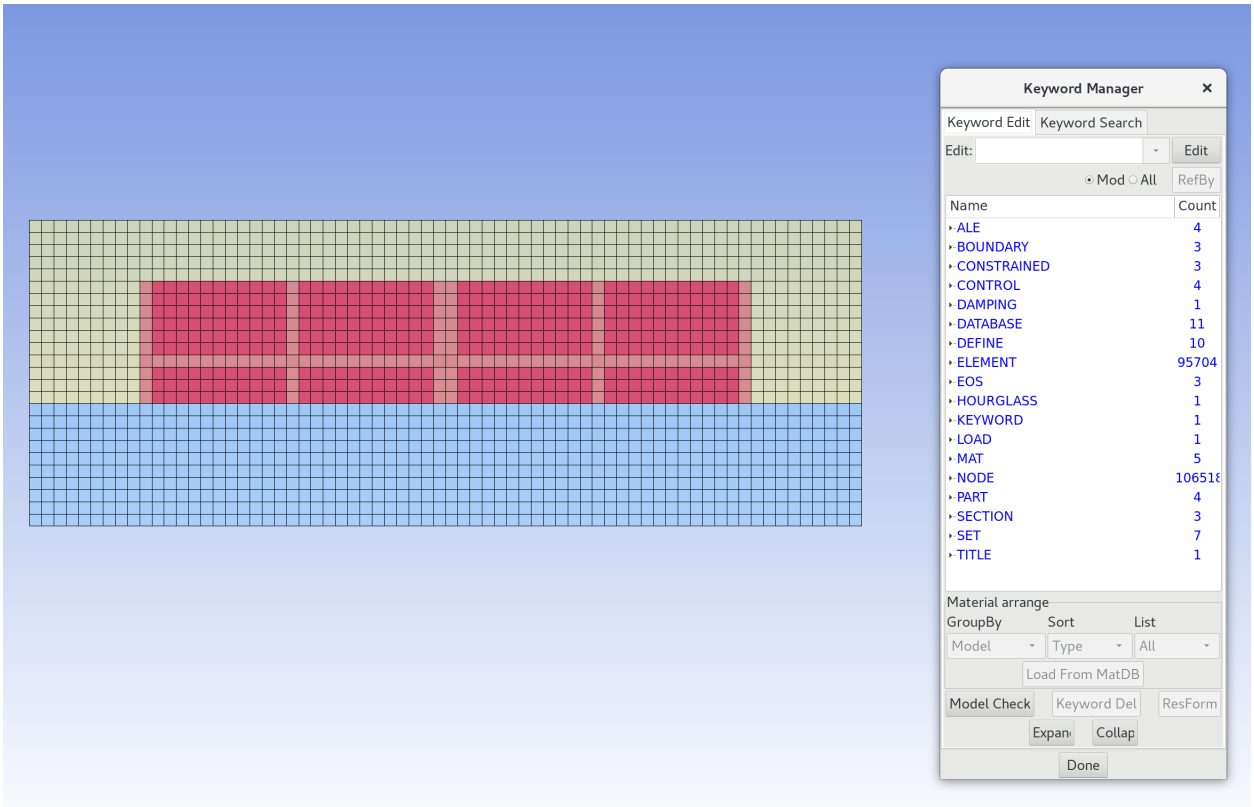

Figure A11. LS-DYNA model for the JAEA small-scale FSIS experiment in elevation view (left) and the modeling features used shown under keyword manager (right)

Figure A12 illustrates the four parts (i.e., water, air, specimen, and water tank) and their sections that are used for modeling the JAEA small scale experimental simulations.

Figure A13 demonstrates the boundary conditions utilized in the simulations. First, SPC boundary conditions are utilized for the gravity initialization by making Z-DOF free so that the model can accommodate earthquake excitations in vertical direction via prescribed motion boundary.

Figure A14 portrays the three contact surfaces i.e., specimen and water, tank and water, and specimen cavity and trapped air which are utilized in simulating JAEA problem. The graphic on the left side of A14 illustrates the numerical values of various types contact parameters used. Figures 15, 16, and 17 illustrate damping parameters, gravity load curve, and earthquake input load curve utilized in the simulations.

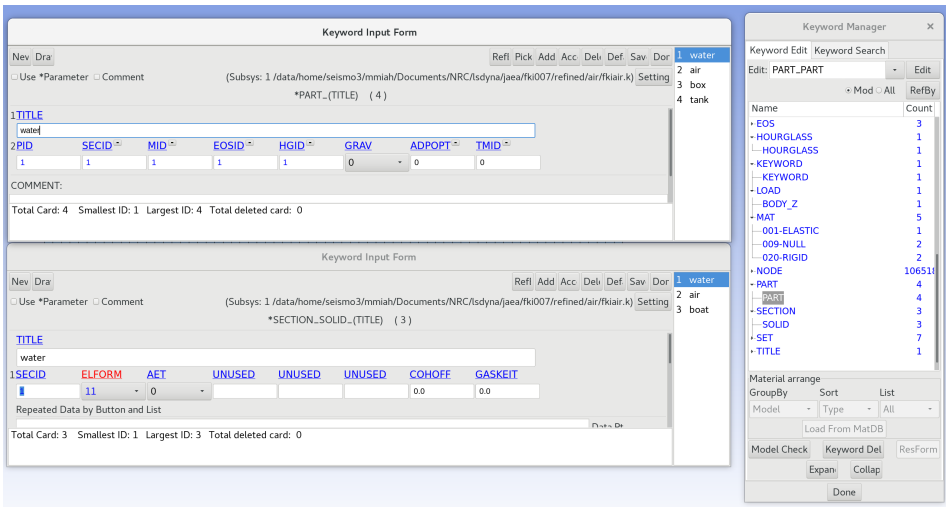

Figure A12. Model parts and sections utilized for the JAEA small-scale experiment simulation.

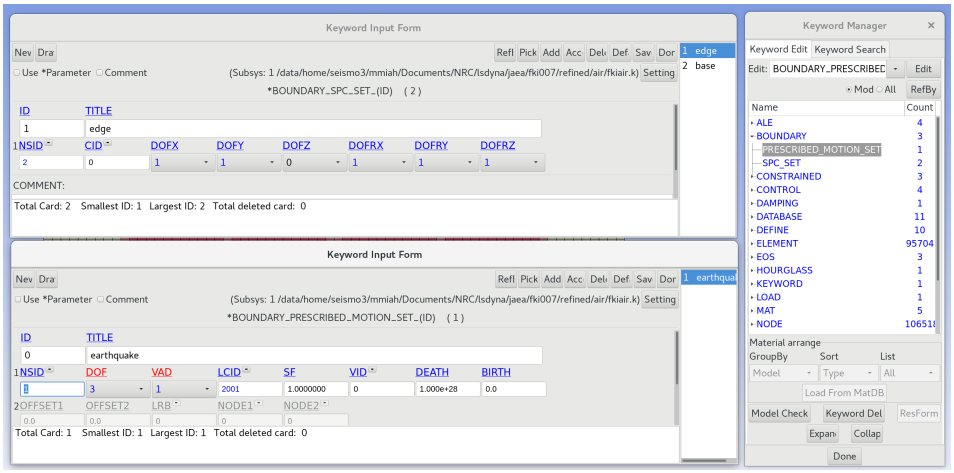

Figure A13. Two types of boundary conditions used for the simulations – SPC for gravity initializations and prescribed motion for the vertical earthquake excitation.

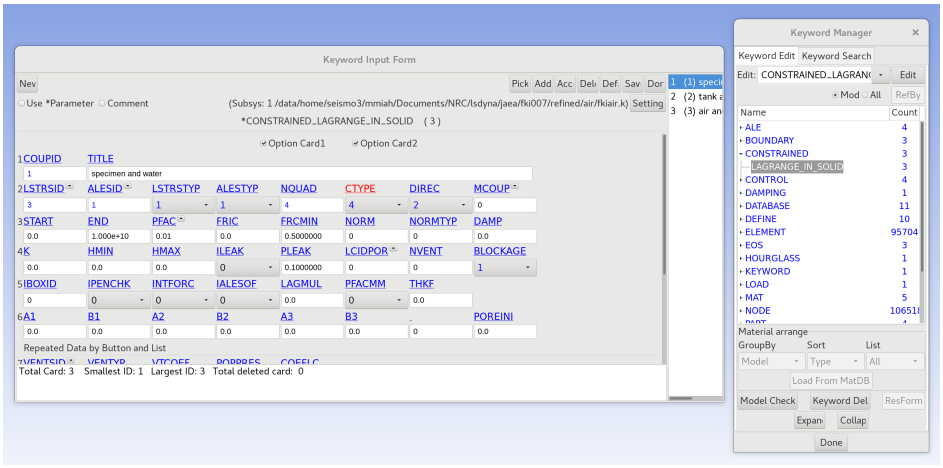

Figure A14. Contact surfaces defined between specimen, air, water, and tank via CONSTRAINED_LAGRANGE_IN_SOLID.

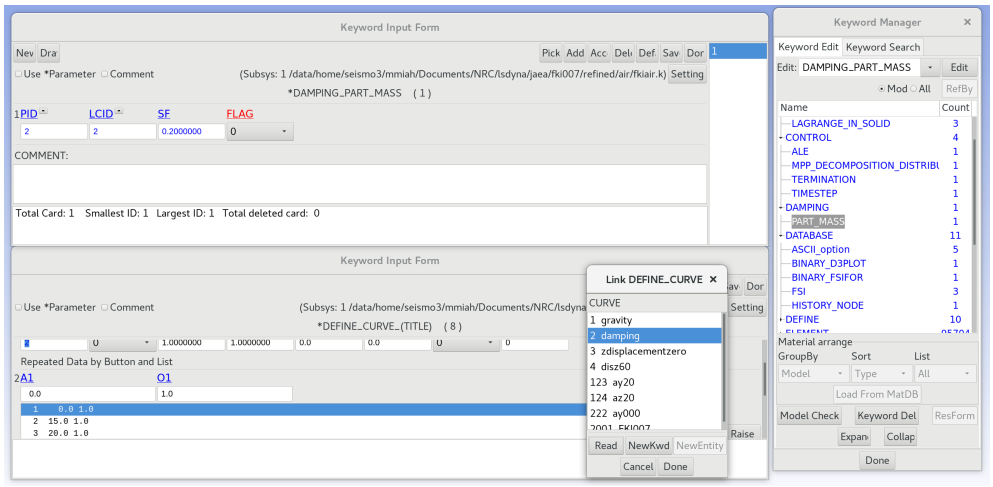

Figure A15. Damping parameters utilized in the model.

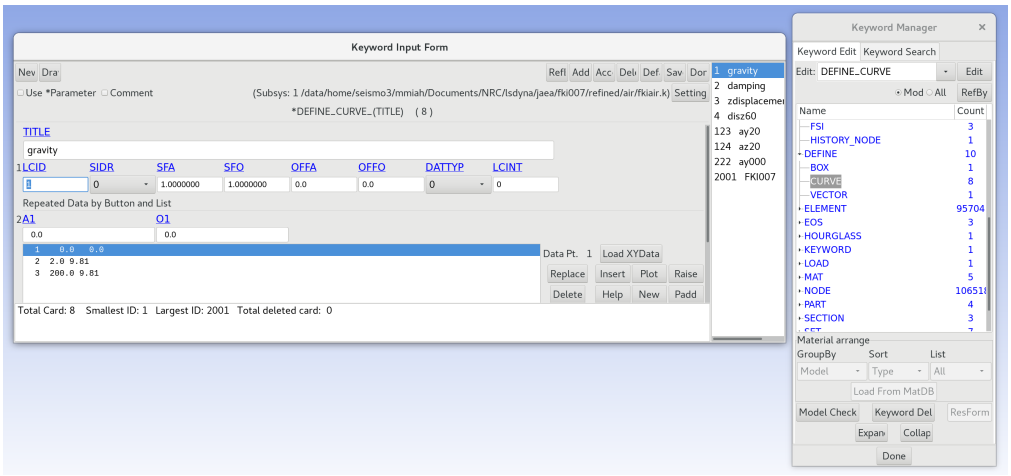

Figure A16. Gravity load curve defined in the JAEA model.

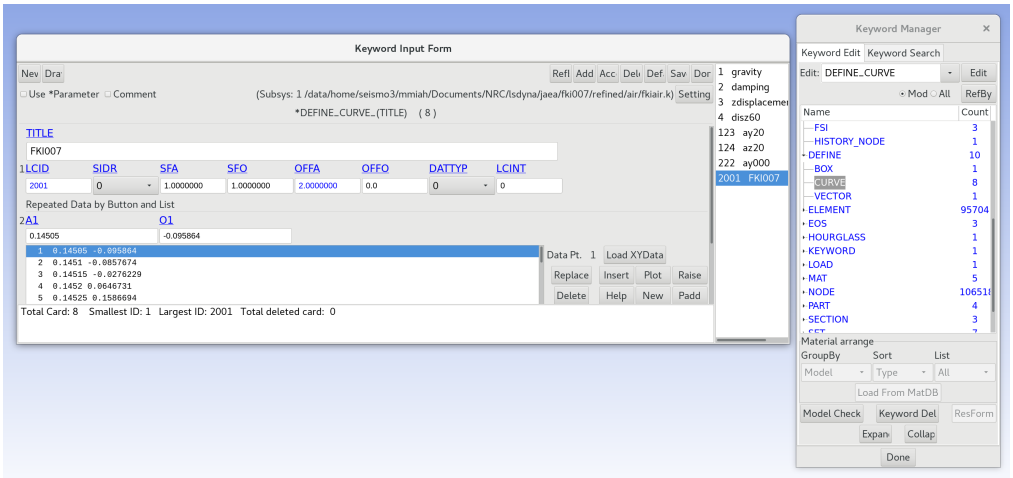

Figure A17. Input earthquake excitation (FKI007) loaded in the model using a load curve ID.

Appendix B – Modeling Features Utilized in OpenSeesPy

OPENSEESPY INPUT PARAMETERS FOR THE BLOCK MODEL FSI SIMULATIONS

There is no GUI interface for OpenSeesPy. The documentation and some example problems are described in the following link:

https://openseespydoc.readthedocs.io/en/latest/index.html

For the FSI system that was analyzed for gravity initialization and earthquake response evaluation, and described in sections 6.4 and 6.5, respectively, the python input file is attached here. For fluid modeling the background meshing scheme is utilized in this simulation.

A python script for analyzing a fluid-structure interaction model subject to earthquake excitation

```
# import the necessary python libraries

import os
from openseespy.opensees import *
import ReadRecord
import pandas as pd

# ------------------------------
# Start of model generation
# ------------------------------

# Create a 2D model with fluid
model('basic', '-ndm', 2, '-ndf', 2)

# Dimensions of the model
L = 200
H = 150
#h = L / 200
h = L / 100
# Number of particles per cell in each direction
numx = 3.0
numy = 3.0

# Fluid properties
rho = 1000
mu = 0.001  #viscosity of water = 0.001
b1 = 0.0
b2 = -9.81
thk = 0.12
kappa = -1.0

# Solid properties
rhos=9e2   # density of the solid material
bf=rhos*b2   # body force per unit volume
```

```
# Total number of particles in each direction
nx = round(L / h * numx)
ny = round(H / h * numy)

# Define wall nodes
node(1, 0.0, L)
node(2, 0.0, 0.0)
node(3, L, 0.0)
node(4, L, L)

# Create fluid particles
eleArgs = ['PFEMElementBubble', rho, mu, b1, b2, thk, kappa]
partArgs = ['quad', 0.0, 0.0, L, 0.0, L, H, 0.0, H, nx, ny]
fluidtag = 10
mesh('part', fluidtag, *partArgs, *eleArgs)

print('num particles =', nx * ny)

# Define nodes for the floating solid block on water surface at the center
#node(5, 88, 164.4)
#node(6, 88, 140.4)
#node(7, 112, 140.4)
#node(8, 112, 164.4)

node(5, 88, 151.6)
node(6, 88, 135.6)
node(7, 112, 135.6)
node(8, 112, 151.6)

# Define solid material properties
#matTag=1
E=1e9
nu=0
nDMaterial('ElasticIsotropic', 1, E, nu, rhos)

# Create mesh for the solid block
sid=2
ndf=2
mesh('line', 1, 2, 5,6, sid, ndf, h)
mesh('line', 2, 2, 6,7, sid, ndf, h)
mesh('line', 3, 2, 7,8, sid, ndf, h)
mesh('line', 4, 2, 8,5, sid, ndf, h)

solidtag=20
eleArgs=['tri31',thk,'PlaneStrain',1,0,rhos,b1,bf]  # (b2=bf) see element(Tri31) command
in OpenSeesPy
```

```
mesh('tri', solidtag, 4, *[1,2,3,4], sid, ndf, 0.5, *eleArgs) # see mesh(quad)

# DOFs for wall mesh nodes
ndf = 2
walltag = 5
wallid = 1
mesh('line', walltag, 4, 1, 2, 3, 4, wallid, ndf, h)

# Description of background mesh
lower = [-0.05*h, -0.05*h]
upper = [L + 2*L, H + 2*H]

# Fix DOFs of the wall nodes to apply uniform acceleration
wallnodes = getNodeTags('-mesh', walltag)
for nd in wallnodes:
    fix(nd, 1, 1)

# Get nodes for the solid body to include in the background meshing scheme
sNodes = getNodeTags('-mesh', solidtag)

# Set some parameters
#record = 'elCentro'
record1 = 'padded_elCentro'
f=open('padded_elCentro.dat', 'r')
df = pd.read_csv(f, sep=",",  names=['time','acc'])
acc=df.loc[:,'acc']
#print (acc)

# Permform the conversion from SMD record to OpenSees record
#dt, nPts = ReadRecord.ReadRecord(record+'.at2', record+'.dat')

# Set time series to be passed to OpenSees uniform excitation
#timeSeries('Path', 2, '-filePath', record1+'.dat', '-dt', 0.02, '-factor', 9.81*3)
timeSeries('Path', 2, '-values', *acc, '-dt', 0.02, '-factor', 9.81*3)

# Create UniformExcitation load pattern
#                       tag dir
pattern('UniformExcitation',  2,   1,  '-accel', 2)

# Employ background meshing for fsi simulation
mesh('bg', h, *lower, *upper, '-wave','oscillation.txt', 1, 25,150,
        '-structure', sid, len(sNodes), *sNodes,
        '-structure', wallid, len(wallnodes), *wallnodes)

# Create constraint object
constraints('Plain')
```

```
# Create numberer object
numberer('Plain')

# Create convergence test object
test('PFEM', 1e-5, 1e-5, 1e-5, 1e-5, 1e-5, 1e-5, 10, 3, 1, 2)

# Create algorithm object
algorithm('Newton')

# Create integrator object
integrator('PFEM', 0.5, 0.25)

# Create SOE object
system('PFEM')
# system('PFEM', '-mumps) Linux version can use mumps

# Set time step size and total simulation time
dtmax = 2e-2
dtmin = 1e-3
totaltime = 50

# Create an analysis object
analysis('PFEM', dtmax, dtmin, b2)

# Save output data for visualization
#recorder('BgPVD', filename, 'disp', 'vel', 'pressure', '-dT', 1e-2)
filename = 'eqfsi'
recorder('BgPVD', filename, 'disp', '-dT', 1e-1)
if not os.path.exists(filename):
   os.makedirs(filename)

time=[]
u8 = []
a8=[]

## Perform a PFEM transient analysis
while getTime() < totaltime:
   # analysis
   if analyze() < 0:
      break
   remesh()
   tCurrent = getTime()
   time.append(tCurrent)
   u8.append(nodeDisp(8,1))
   a8.append(nodeAccel(8,1))
```

```
            #break

        ## Write displacement result output to a file
        f=open('nodeaccel.txt', 'w')
        for item in zip(time, a8):
                f.write(str(item).strip("()")+'\n')

        ## Write displacement result output to a file
        f=open('nodedisp.txt', 'w')
        for item in zip(time, u8):
    f.write(str(item).strip("()")+'\n')


## End
```

Appendix C – Examples of Long Period Ground Motions at Large Distances from the Causative Fault

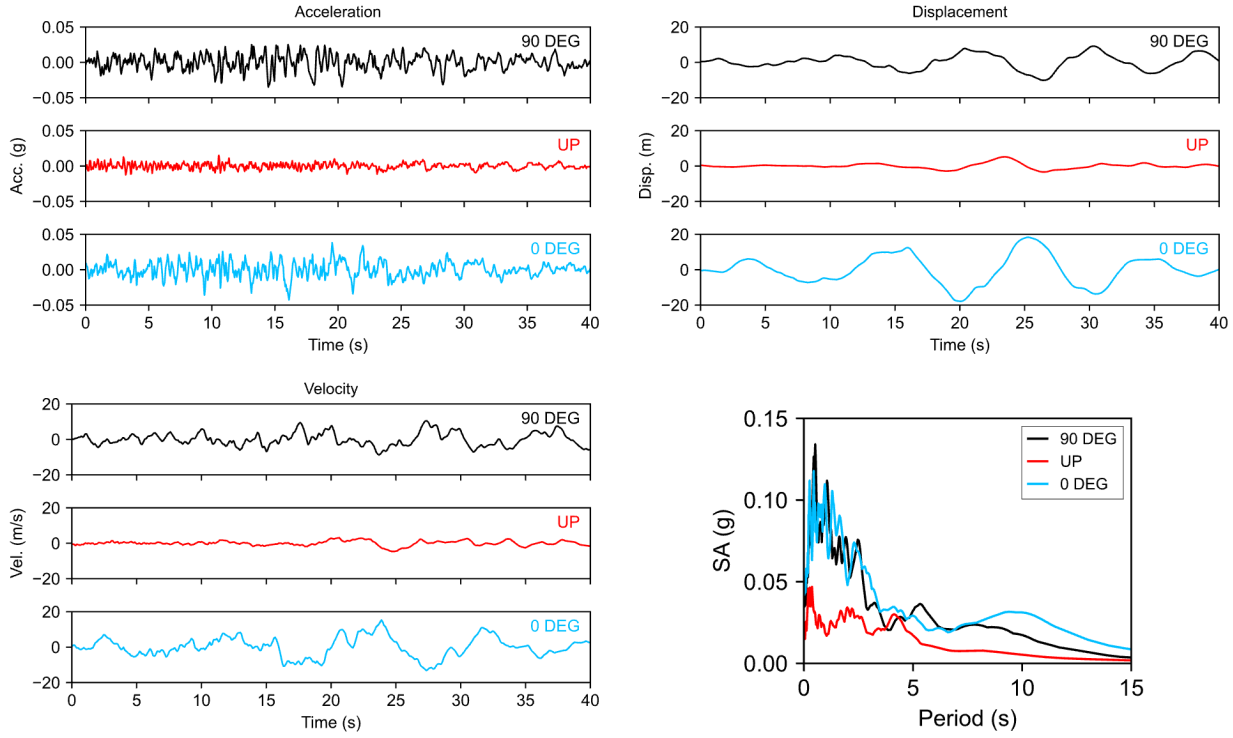

Figure C1. Observed motions for the M 7.3 Landers CA earthquake at Inglewood CA Union Oil yard at ~158 km from the causative fault (California Geological Survey station 14196).

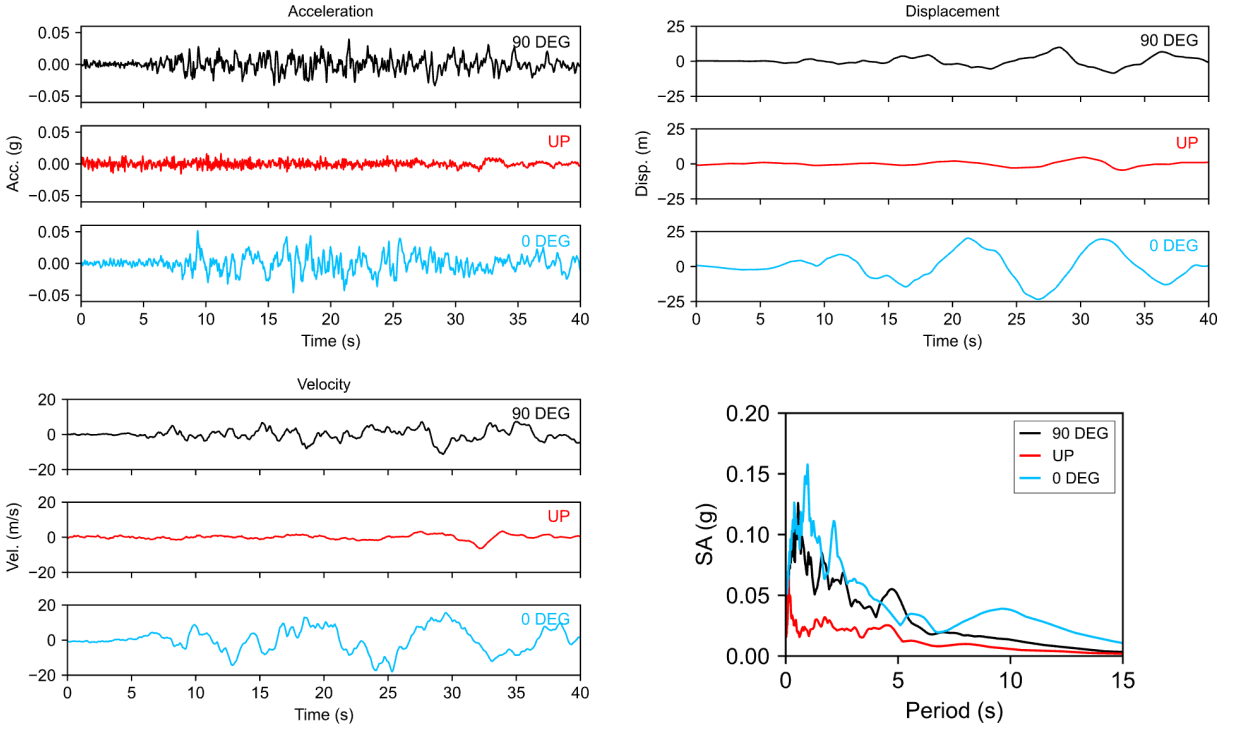

Figure C2. Observed motions for the M 7.3 Landers CA earthquake at Downey CA county maintenance building at ~167 km from the causative fault (California Geological Survey station 14368).

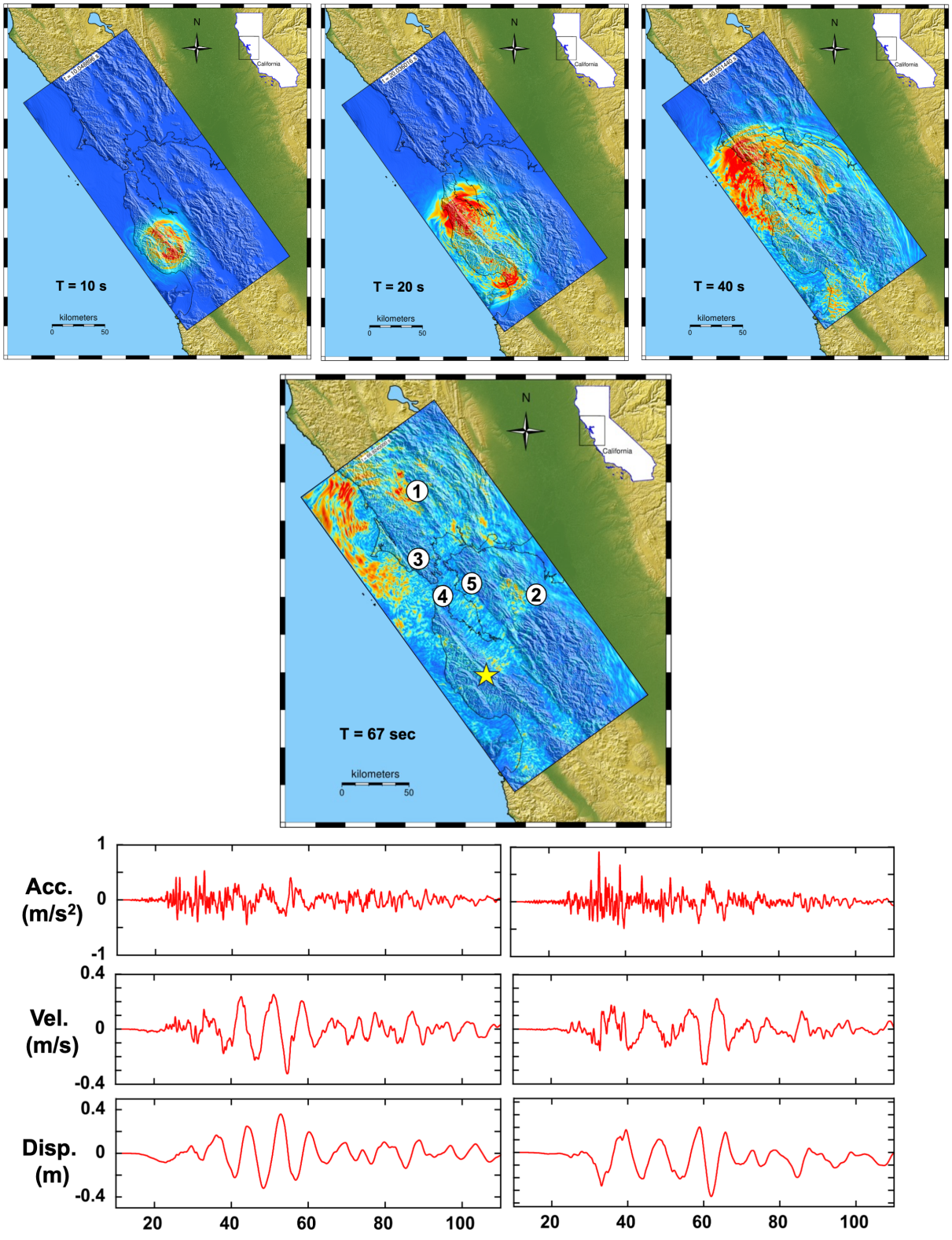

Figure C3. Simulated ground motions in the Livermore Valley (site 2) for a M 7.5 San Andreas fault earthquake [29].